EFFECTS OF NITRIC OXIDE ON CALCIUM-INDUCED SKELETAL MUSCLE ATROPHY

By

ELIZABETH HENDERSON ZEANAH

A THESIS PRESENTED TO THE GRADUATE SCHOOL
OF THE UNIVERSITY OF FLORIDA IN PARTIAL FULFILLMENT
OF THE REQUIREMENTS FOR THE DEGREE OF
MASTER OF SCIENCE

UNIVERSITY OF FLORIDA

2009

To my parents, whose absence has not diminished their influence

ACKNOWLEDGMENTS

First and foremost, I thank my advisor Dr. David Criswell for his support, kindness, and patience during my time as a graduate student in his laboratory. Dr. Criswell's loyalty and integrity as a mentor have been as impactful on my graduate studies as has been his scientific guidance. I also thank my committee members, Drs. Scott Powers and Stephen Dodd for their support. Their dedication to and passion for skeletal muscle research, expressed through their own research, teaching, and publications, have been instrumental in developing my interest and expertise in this area. Additionally, I thank my doctoral program advisor Dr. Randy Braith for his support of my concurrent work in Dr. Criswell's laboratory and the completion of this project.

Second, I would like to thank Dr. Quinlyn Soltow, formerly of the Molecular Physiology lab, for her invaluable instruction and guidance throughout all phases of this project. Her assistance and input greatly benefitted not only this project but also the development of my skills as an independent scientist - nearly everything I know about benchwork I owe to Dr. Soltow. But above all else I thank her for being my friend. I also would like to acknowledge all of the current and past members of the Molecular Physiology lab, particularly Dr. Vitor Lira for his advice regarding L6 cell culture and assistance in the lab.

Finally, I thank my family and friends for their support over the past three years. I would not have had the strength and motivation to pursue this degree through some of the most difficult of adversities were it not for their love and encouragement.

TABLE OF CONTENTS

LIST OF FIGURES

LIST OF ABBREVIATIONS

A23187	calcimycin, calcium ionophore A23187
Akt	Akt/protein kinase B
ATP	adenosine triphosphate
ATPase	adenosine triphosphatase
Ca^{2+}	calcium ion
DETA-NO	diethylenetriamine NONOate
DMSO	dimethyl sulfoxide
EDTA	ethylenediaminetetraacetic acid
eNOS	endothelial nitric oxide synthase
FOXO	forkhead box O
IGF-1	insulin-like growth factor-1
iNOS	inducible nitric oxide synthase
L-NMMA	L-N^G-monomethyl arginine citrate
MAFbx	muscle atrophy F-box
MuRF1	muscle ring finger-1
nNOS	neuronal nitric oxide synthase
NO	nitric oxide
NOS	nitric oxide synthase
PAPA-NO	propylamine propylamine NONOate
PBS	phosphate-buffered saline
PI3K	phosphoinositide-3-kinase
PVDF	polyvinylidene difluoride
TBS	tris-buffered saline

Abstract of Thesis Presented to the Graduate School
of the University of Florida in Partial Fulfillment of the
Requirements for the Degree of Master of Science

EFFECTS OF NITRIC OXIDE ON CALCIUM-INDUCED SKELETAL MUSCLE ATROPHY

By

Elizabeth Henderson Zeanah

December 2009

Chair: David S. Criswell
Major: Applied Physiology and Kinesiology

Skeletal muscle atrophy occurs as a result of long periods of disuse, as seen with bedrest, limb immobilization, and space flight; and disease, as seen with cancer, sepsis, and metabolic dysfunction. Atrophy proceeds via different mechanistic pathways among these conditions, but in most cases, including disuse, levels of intracellular calcium increase in the muscle cells. This rise in intracellular calcium stimulates calpain activation and subsequent protein degradation, or proteolysis. Calpain cleaves the structural proteins that hold the sarcomere together, thereby releasing the contractile myofibrillar proteins for proteasome degradation; this is thought to be the rate-limiting step in skeletal muscle proteolysis because the proteasome cannot degrade intact sarcomeres. Little is known about the regulation of calpain activity, however, nitric oxide has been proposed as a possible mediator. This study used the calcium ionophore calcimycin to increase intracellular calcium and induce calpain activity in L6 myotubes. It is the first to examine the effects of exogenous nitric oxide on calpain activity in mature myotubes and to demonstrate a dose-dependent protective role for nitric oxide on calpain targets and concurrent prevention of myotube atrophy. Nitric oxide attenuated calpain cleavage of the structural protein talin and reduced visible myotube atrophy. Therefore, moderate doses of nitric oxide can prevent protein degradation and atrophy following a calcium challenge in L6 myotubes.

CHAPTER 1
INTRODUCTION

Background

Skeletal muscle atrophy can result from a variety of conditions, such as prolonged bed rest, limb immobilization, denervation, cancer, sepsis, aging, malnutrition, metabolic dysfunction, and space flight. Skeletal muscle atrophy is a clinically-significant problem not only because it is a common complication and/or outcome of these conditions but also because it can contribute to the onset or worsening of others. Loss of muscle mass is a primary cause of decreased mobility and balance, which can lead to inactivity, injury, and inability to perform daily tasks, as well as contribute to metabolic syndrome (obesity, hyperlipidemia, hypertension, and insulin resistance) and increased risk for type II diabetes and cardiovascular disease.

While there are several different molecular pathways through which skeletal muscle atrophy can occur depending upon the atrophy stimulus, elevated intracellular Ca^{2+} occurs in most atrophic conditions. The role of Ca^{2+} is especially critical to understanding disuse atrophy because Ca^{2+} levels greatly increase with disuse (10). The mechanism for this rise in Ca^{2+} is unknown, but increasing oxidative stress may play a major role (27). Elevated intracellular Ca^{2+} is a powerful atrophy signal because Ca^{2+} stimulates calpain activity. Calpains are Ca^{2+}-dependent cysteine proteases that cleave the intermediate filaments of the sarcomere to release actin and myosin for degradation by the proteasome (6). Calpains cannot degrade contractile proteins, but, because myofibrillar release must precede proteasome proteolysis, calpain activity is often cited as the rate-limiting step in proteolysis (27). In fact, evidence from rat diaphragm muscle shows that calpains may be necessary for protein degradation by the proteasome (31). Interestingly, the same study has presented evidence that calpain activity inhibits protein synthesis via the IGF-1/Akt pathway, suggesting a dual role for calpains in muscle atrophy (31).

Little is known about the regulation of calpain activity. However, a small number of research studies have suggested NO as a possible mediator. NO has been shown to inhibit calpain activity in human neutrophils (22) and rat cardiac myocytes (5). Evidence in skeletal muscle is limited to date. In C2C12 myotubes, mechanically-induced endogenous NO release has been associated with increased intact intermediate filaments known to be cleaved by calpains (42). And in C2C12 myoblasts, induction of calpain activity with A23187 produced intermediate filament cleavage, and this activity was attenuated by exogenous NO (19). This is the strongest evidence to date of a protective role for NO in calpain proteolysis in skeletal muscle. However, this relationship has not yet been established in mature myotubes and has not been connected with other atrophy markers.

Thus, several questions remain regarding the role of NO in regulating calpain activity in skeletal muscle. First, it is unknown if exogenous NO will directly inhibit calpain action in mature myotubes. Second, it is unknown whether or not the effects of NO are dose-dependent. Third, even if exogenous NO does decrease the cleavage of intermediate filaments by inhibiting calpains, it has not been clearly established that this prevents muscle atrophy (loss of myotube size and/or total protein). None of the aforementioned studies has presented clear evidence of atrophy in connection with calpain induction or prevention of atrophy with an increase in NO. While this relationship between calpain proteolysis and muscle atrophy may seem obvious, it is possible that at least some of the calpain activity is devoted to cellular remodeling. Thus, evidence of myotube atrophy and/or activity of other atrophy-associated proteins, such as the proteasome E3 ligases MAFbx and MuRF1, are needed in conjunction with evidence of calpain proteolysis and NO effects.

Specific Aims and Hypotheses

Specific aim 1: To test that elevated intracellular Ca^{2+} levels induced by treatment with A23187 is a dose-dependent model of skeletal muscle atrophy stimulating calpain proteolysis of intermediate filaments and increasing molecular markers of proteasome activity and to determine whether or not exogenous NO can attenuate these effects.

Hypothesis 1A: Elevation of intracellular Ca^{2+} by treatment with A23187 causes increased proteolysis of intermediate filaments (e.g. talin) by calpain and increased proteasome activity (e.g. FOXO3a, MAFbx).

Hypothesis 1B: Exogenous NO administration attenuates calpain proteoloysis and proteasome activity after treatment with A23187.

Specific aim 2: To test if elevated intracellular Ca^{2+} by treatment with A23187 induces myotube atrophy (loss of size and/or total protein) and whether or not exogenous NO administration results in decreased atrophy.

Hypothesis 2A: Elevation of intracellular Ca^{2+} by treatment with A23187 causes myotube atrophy.

Hypothesis 2B: Exogenous NO attenuates myotube atrophy after treatment with A23187.

Clinical Significance

Skeletal muscle accounts for approximately 40% of human body mass and is required for basic functions such as locomotion, respiration, metabolism, and thermoregulation. Skeletal muscle responds to the presence or absence of stimuli with changes in protein synthesis, protein degradation, or both. When the rate of protein degradation surpasses the rate of protein synthesis, skeletal muscle atrophy occurs. Atrophy is described as a loss in muscle fiber size, protein content, and strength. An increase in protein degradation and subsequent muscle atrophy can occur due to periods of inactivity, lack of nutrition, aging, or disease and can

contribute to numerous disease states. A loss of skeletal muscle leads to fatigability, decreased mobility and ability to execute daily activities, and insulin resistance, all of which are risk factors for type II diabetes and cardiovascular disease. Skeletal muscle loss is also a complication in cancer and cancer therapies.

Much work has been done in the field of skeletal muscle atrophy. Various models, including limb immobilization, limb unloading, denervation, and endotoxin administration, have been used to research the causes of muscle atrophy. These models are all performed *in vivo*; they can provide little insight on the intrinsic factors leading to muscle degradation and are heavily influenced by many neural and humoral factors. Therefore, it is necessary to study skeletal muscle atrophy *in vitro* to investigate the signaling pathways leading to loss of muscle mass and what might attenuate atrophy signaling. Elucidating these signals and what mediates them may lead to therapeutic strategies, such as pharmaceutical interventions, to attenuate or eliminate skeletal muscle atrophy as a complication and cause of disease, which could dramatically improve both longevity and quality of life.

Strengths and Limitations

The primary strength of this *in vitro* study is the high level of experimental control exercised over the muscle cells. Unlike *in vivo* studies, this study was not subject to influence by the many humoral and neural factors that would be confounding in a whole animal. Although *in vitro* studies require confirmation *in vivo*, this study provides one piece of the cellular signaling puzzle that would be impossible to ascertain without *in vitro* experimentation that eliminates other physiological factors. Furthermore, this is the first study of calpain proteolysis and NO mediation that examines not only molecular signals associated with proteolysis but also the degree of atrophy in the myotubes.

This study used A23187 to induce skeletal muscle atrophy because elevated intracellular Ca^{2+} is a common element in most, if not all, models of skeletal muscle atrophy and is particularly characteristic of disuse atrophy (10). While this stimulus is a useful simulation of skeletal muscle atrophy in general, this model cannot be equated with a specific atrophy stimulus. And although myotube atrophy was induced and a dose-response experiment revealed a trend of increasing atrophy signals with A23187, it is not certain exactly which atrophy pathways were activated. This study examined talin cleavage as an indirect measure of calpain activity, MAFbx expression as an indicator of proteasome activity, FOXO3a as a stimulator of MAFbx transcription, and Akt phosphorylation as an inhibitor of FOXO3a activity. However, elucidating all of the pathways involved was beyond the scope of this study.

Additionally, it is possible that some of the atrophy signals were missed due to the time points selected for study. Cellular protein was harvested after 60 minutes of incubation with A23187 based upon previous evidence that proteasome activity in L6 myotubes increases most rapidly during the first 40 minutes of incubation with A23187 and then continues to increase significantly for 120 minutes (21). It was believed that 60 minutes would be sufficient time to see proteasome activity but still brief enough not to miss evidence of the calpain cleavage that should precede it. Incubating for a longer period would have risked losing the cleaved talin protein to proteasome degradation, and since this study was primarily concerned with calpain activity in this study, the time was limited to 60 minutes. However, experiments done to show myotube atrophy were conducted for both 24 and 48 hours, demonstrating that the effects of A23187 and NO were not transient.

CHAPTER 2
LITERATURE REVIEW

Skeletal muscle atrophy is a clinically significant problem as it arises from a variety of factors, such as prolonged bed rest, limb immobilization, space flight, denervation, cancer, sepsis, and ageing. Loss of muscle mass has been shown to contribute to inactivity, obesity, insulin resistance, hypertension, and hyperlipidemia (altogether termed metabolic syndrome). Minimization of muscle atrophy and its side effects will prevent the progression to more serious pathological disorders such as metabolic disease and loss of functional independence and overall quality of life.

Overview of Skeletal Muscle Atrophy

During atrophy the rate of protein degradation exceeds the rate of protein synthesis. Both degradation and synthesis are highly complex, intricately regulated cellular processes that can occur via many interdependent pathways. However, it is generally accepted that in muscle atrophy, the increase in proteolysis has a greater impact than protein synthesis (27). There are four major proteolytic systems in skeletal muscle: lysosomes, proteasomes, caspases, and calpains.

Role of Lysosomes

Lysosomes are highly-acidic, membrane-bound vesicles containing proteases, lipases, phosphatases, and other catabolic molecules. The dominant lysosomal proteases are cathepsins L, B, D, and H (2). Although these cathepsins are found in all tissues, the relative degree of their expression is highly correlated with the tissue's inherent rate of protein turnover (2). Because skeletal muscle has a relatively low rate of protein turnover, cathepsin concentrations are relatively low in skeletal muscle (2). This may explain, at least in part, why cathepsins seem to have a small role in skeletal muscle atrophy. Inhibition of lysosome and/or cathepsin activity

does not significantly attenuate either proteolysis or atrophy (9, 34, 37). Similar evidence suggests that the cathepsins do not degrade myofibrils but rather are responsible for degrading membrane proteins (18). While the import of membrane proteolysis cannot be dismissed, this action is not sufficient to produce atrophy.

However, several experiments have shown that cathepsin mRNA expression and/or cathepsin activity increase(s) during disuse atrophy (reviewed in ref. 18). This may be evidence of cell maintenance and healthy protein turnover. Lysosomes are important mediators of autophagy, which is a mechanism for removal of old or damaged cellular proteins or organelles. In this process, proteins or cellular components targeted for removal are imported into, or engulfed by lysosomes. Although autophagy is important in striated muscle, recent evidence shows that increased autophagy is associated with improved cellular function and protection against age-associated atrophy (3, 18).

Thus, we can conclude that the lysosomal proteases are significant yet minor players in skeletal muscle atrophy and may even protect against age-associated atrophy. Since they do not appear to degrade the myofibrils, a more dominant system must be involved in atrophic proteolysis.

Role of Proteasomes

Proteasomes are generally accepted to be responsible for the bulk of skeletal muscle proteolysis because they degrade the contractile myofibrillar proteins (i.e. actin and myosin) (18, 27). Protein degradation by the proteasomes can occur in two ways. First, the 26S proteasome can degrade ubiquitinated proteins in an energy-dependent process. The 20S proteasome, however, can degrade proteins in an energy-and ubiquitin-independent process.

Ubiquitin-dependent proteolysis

Ubiquitin-dependent proteolysis requires ATP and the synergistic action of the two components of the 26S proteasome: the 20S proteolytic core and the 19S regulatory subunits. The 26S proteasome is made up of a 20S proteasome and 19S regulatory subunits with the high ATPase activity necessary for energy-dependent proteasome action (26, 27, 35). These 19S complexes are responsible for recognizing and binding ubiquitinated proteins, removing the ubiquitin chain through ATP hydrolysis, and transferring the protein into the 20S proteasome core for passive degradation (27, 35).

Ubiquitin is a protein that covalently bonds to targeted proteins through an ubiquitin-protein ligating system (35). This system consists of an ubiquitin-activating enzyme (E1), several ubiquitin-conjugating enzymes (E2), and substrate-specific ubiquitin-ligating enzymes (E3) (17). All three enzymes are required for ubiquitin-proteasome action. At least one ubiquitin-conjugating enzyme, $E2_{14k}$, is significant in regulating skeletal muscle proteolysis (20). However, because the E3 enzymes are responsible for selective protein recognition and are substrate-specific, they appear to be especially important in the regulation of tissue-specific atrophy (13, 35).

Atrophy-associated E3 ligases and relationship with the IGF-1/Akt pathway via FOXO

While many E3 ubiquitin-ligating enzymes have been identified, the gene expressions of two specific E3s have been identified as being up-regulated during skeletal muscle atrophy: MuRF1 and MAFbx, also known as atrogin-1 (12). These genes are particularly significant because they are up-regulated in nearly all models of atrophy, including unweighting, immobilization, denervation, cachexia (4), starvation (15), and sepsis (41). Both MAFbx and MURF-1 have been implicated in at least 13 atrophy models, including models of disuse (4, 13), but their upregulation can be antagonized by simultaneous treatment with IGF-1 (28) acting

through the PI3K/Akt pathway (29, 33). This suggests a novel role for Akt inhibition of atrophy signaling. The mechanism by which Akt inhibits MAFbx and MuRF1 upregulation involves the FOXO family of transcription factors (29, 33). FOXO transcription factors are excluded from the nucleus when phosphorylated by Akt and translocate upon dephosphorylation. The translocation of FOXO is required for upregulation of MuRF1 and MAFbx and is sufficient to induce atrophy (30).

Ubiquitin-independent proteolysis

Recent evidence supports the existence of an ubiquitin-independent proteolytic process as well. The 20S proteasome can recognize and degrade oxidized proteins without the 19S subunits and ubiquitin-ligase chain (16). Furthermore, this pathway obviates the need for ATPases because 20S proteosome degradation is a passive process (16, 27). These findings suggest that oxidative stress is a mediator of skeletal muscle atrophy driven by the proteasome system (27).

Limitations of the proteasome system

Because of their collective ability to degrade the contractile proteins, the proteasomes are responsible for the bulk of skeletal muscle proteolysis. However, proteasomes cannot degrade intact sarcomeres (14). Since the majority of muscle proteins are contained within these acto-myosin complexes, there must be additional pathways by which the myofibrils are released prior to proteasome degradation (36). This "myofibrillar release" is performed by two interrelated but distinct Ca^{2+}-dependent proteolytic systems: caspases and calpains.

Role of Caspases

Caspases are Ca^{2+}-dependent cysteine proteases capable of cleaving the intermediate filaments of the sarcomeres and releasing myofibrils for degradation by the proteasomes (8, 14, 36). Furthermore, inhibition of caspase-3 prevents actin accumulation in the cytosol, indicating that caspase-3 is a necessary first step for skeletal muscle proteolysis (8).

However, caspases are best known for their role in triggering apoptosis (6). Apoptosis results in a loss of myonuclei (and likely myofiber size as a result) and occurs through at least three known pathways: sarcoplasmic reticulum, receptor-mediated, and mitochondrial (reviewed in ref. 27).

Caspase Regulation and Calpains

In the sarcoplasmic reticulum pathway, another proteolytic system, the calpains, partially mediates caspase activity. When the sarcoplasmic reticulum is injured, the regulation of Ca^{2+} release and sequestration is impaired, and Ca^{2+} accumulates in the cytosol (27). The high level of Ca^{2+} activates both caspase-7 and calpain, either of which can begin a caspase cascade leading to nuclear damage and subsequent apoptosis (27). So, calpain activation appears to promote caspase apoptotic activity. Also, caspase expression appears to enhance calpain activity by serving as a substrate for calpastatin, the only endogenous inhibitor of the calpains (reviewed in a subsequent section). Thus, when caspases are highly expressed, calpastatin activity will decrease as it binds to caspase substrates, and calpain activity will then increase in the absence of its inhibitor. Calpains, the fourth proteolytic system in skeletal muscle, are fully dicussed in the following section.

Overview of Calpains

Calpains, like caspases, are Ca^{2+}-dependent cysteine proteases that cleave the intermediate filaments of the sarcomere to release actin and myosin for proteasome degradation (6). They are ubiquitously expressed in all mammalian cells, but some isoforms are tissue-specific (6). Calpains cannot degrade contractile proteins but, because this myofibrillar release must precede proteasome proteolysis, calpain activity is often cited as the rate-limiting step in proteolysis (27). (Recent literature has also proffered non-proteolytic roles of the calpains as well, including

involvement in proliferation, differentiation, migration, and gene expression, but these are beyond the scope of this review.)

Calpains appear to be necessary for proteasome protein degradation. Recent ex vivo experiments in the rat diaphragm showed that calpain activation increased total proteolysis by 65% and proteasome-dependent proteolysis by an impressive 144% (31). In the same experiments, inhibiting the proteasome during calpain activation prevented this increase in proteolysis (31). Taken together, this data supports the theory of sequential proteolysis just described and illustrates the necessity of both calpains and proteasomes in skeletal muscle atrophy. Interestingly, calpain activity concurrently inhibited protein synthesis via the IGF-1/Akt pathway, suggesting a dual role for calpains in muscle atrophy (31).

At least 15 distinct calpain isoforms have been identified (6). Skeletal muscle expresses three dominant isoforms: calpain 1 (μ-calpain), calpain 2 (m-calpain), and calpain 3 (p94) (1, 6, 38). Calpains 1 and 2 are implicated in skeletal muscle atrophy (1, 6, 27, 32) and exist as heterodimers (6).

Regulation of Calpains

Although the regulation of calpains has yet to be fully elucidated, intracellular Ca^{2+} and calpastatin have been shown to exert great influence over calpain activity.

Intracellular Ca^{2+}

Intracellular Ca^{2+} is a powerful stimulator of calpain activity. As intracellular Ca^{2+} concentrations rise, calpain moves to the plasma membrane for activation. There, Ca^{2+} and membrane phospholipids activate the calpain heterodimer, which than dissociates into active calpain 1 and calpain 2 (6).

The role of Ca^{2+} is critical to understanding disuse atrophy because Ca^{2+} levels increase with disuse (10). The mechanism for this rise in Ca^{2+} is unknown, but increasing oxidative stress

may play a major role (27). Reactive oxygen species can damage cellular membranes and the sarcoplasmic reticulum, increasing permeability and Ca^{2+} leakage (10, 27). Ca^{2+} may also leak from the mitochondria, worsening the problem (10). So, the high levels of intracellular Ca^{2+} seen during disuse atrophy support the idea that calpains are crucial contributors in these atrophy models.

However, the levels of Ca^{2+} needed to achieve half-maximal proteolysis by calpain 1 and calpain 2 are much higher than physiological Ca^{2+} levels (38). During normal function, the sarcoplasmic reticulum maintains Ca^{2+} concentrations at approximately 10^{-7} M (11). And even during atrophy, Ca^{2+} concentrations are unlikely to reach the 0.2-1 mM needed to activate calpain 2 or even the 2-75 μM needed for calpain 1 activation (6, 38). But Ca^{2+} somehow still activates calpains as evidenced by the strong body of literature supporting calpain proteolysis. Several hypotheses have been offered to explain physiological Ca^{2+} activation of calpain, including increased Ca^{2+} affinity *in vivo* due to interaction with calpain activator proteins (6). The exact mechanism for calpain activation in relatively low Ca^{2+} concentrations, however, remains unknown.

Calpastatin

Calpastatin is the only known endogenous inhibitor of calpain (36). Calpastatin binds to calpain and thereby prevents it from cleaving the intermediate filaments (26). So, calpain activity appears to be mediated by a balance between intracellular Ca^{2+} concentrations and calpastatin expression.

Calpastatin has been used to study calpain activity in many atrophy models. Transgenic mice that overexpress human calpastatin significantly increased soleus and extensor digitorum longus muscle mass in ex vivo experiments (24). During hindlimb unloading, overexpression of

calpastatin reduced muscle atrophy by a significant 30% (36). This evidence points to not only the power of calpastatin as an inhibitor but also the requisite role of calpain activity in muscle atrophy.

Overview of NO Production in Skeletal Muscle

NO is a gaseous free radical with many biological effects. Due to its high chemical reactivity, NO can be a powerful signaling molecule and antioxidant or can be harmful through the nitrosylation of many proteins. NO is produced physiologically by the transformation of L-arginine by three NOS isoforms; all three isoforms catalyze the formation of NO from L-arginine, oxygen, and NADPH. In skeletal muscle, two isoforms are constituitive: eNOS and nNOS (23). The third isoform, iNOS, is induced by cytokines and is only transiently active in skeletal muscle (23, 39).

eNOS and nNOS are activated to produce NO during both mechanical loading and activity (32, 39, 42). To acquire the active state, eNOS and nNOS also require calmodulin (CaM) and Ca^{2+}, indicating that NO synthesis is triggered by an elevation of intracellular Ca^{2+} and that activity-induced NO production, in particular, is stimulated by Ca^{2+}. It is important to note that although Ca^{2+} also stimulates calpain activity, the intracellular Ca^{2+} accumulation during normal activity and/or exercise is transient and therefore insufficient to promote Ca^{2+}-dependent proteolysis (reviewed in ref. 11). Therefore, it is still possible that muscle activity/ Ca^{2+}-dependent nitric oxide release could attenuate calpain activity.

Evidence for NO as a Potential Regulator of Calpains

A limited number of studies have proposed NO as a potential regulator of calpain activity. It is difficult to draw conclusions based on the results of these studies because they vary with respect to the source of NO, the *in vitro* techniques used, the species used (human, rat, mouse), and the tissue types studied.

Tissues Other than Skeletal Muscle

A decade ago Michetti et al. were the first to establish a direct connection between calpain and nitric oxide with work in human neutrophils, demonstrating that NO donor sodium nitro-prusside blocked nearly all calpain 2 activity but had little effect on calpain 1 (22). Although this work was not done in skeletal muscle, it is possible that the similar effects could be seen across tissue types.

More recently other evidence of nitric oxide inhibition of calpain activity has been shown in cardiac myocytes. Chohan et al. discovered that exogenous L-arginine administration restored SR function in intact, isolated ischemia-reperfused rat hearts by preventing calpain activation (5). Although claiming calpain inhibition as the cause of the SR restoration is tenuous due to measurement from muscle homogenate, this study provides at least a promising indication of nitric oxide's ability to inhibit calpains.

Skeletal Muscle

Research of NO inhibition of calpains in skeletal muscle is so far very limited. In 2004, Zhang et al. showed that stretch-induced increases in nNOS expression and endogenous NO release were associated with increased intact talin and vinculin, two intermediate filaments known to be cleaved by calpains, and decreased cleaved/total talin ratio (42). This study suggested that NO both up-regulated talin expression in response to mechanical loading and down-regulated cleavage of talin by inhibiting calpain activity (42). However, it is important to note that calpain inhibitors were not used in the protein expression analysis (although calpain inhibition appeared to have an impact on elastic modulus), so it is possible that NO-induced up-regulation of intermediate filament expression, and not inhibition of degradation by calpains, was responsible for the changes.

Also recently, Koh and Tidball administered the Ca^{2+} ionophore A23187 to C2C12 myoblasts to induce calpain activity and showed that the NO-donor SNP prevented proteolysis of talin (19). The inhibition of calpain action by NO approximated the inhibition caused by a known calpain inhibitor (19). This is the strongest evidence to date of a protective role for NO in calpain proteolysis in skeletal muscle. However, this relationship has not yet been established in mature myotubes and has not been connected with other atrophy markers.

Several questions then remain regarding the role of NO in regulating calpain activity in skeletal muscle. First, it is unknown if exogenous NO will directly inhibit calpain action in mature myotubes. Second, it is unknown whether or not this protective effect is dose-dependent. Third, even if exogenous NO does decrease the cleavage of intermediate filaments by inhibiting calpains, it has not been clearly established that this prevents muscle atrophy (loss of myotube size and/or total protein). None of the aforementioned studies has presented clear evidence of atrophy in connection with calpain induction or prevention of atrophy with an increase in NO. While this relationship between calpain proteolysis and muscle atrophy may seem obvious, it is possible that at least some of the calpain activity is devoted to cellular remodeling. Thus, evidence of visible myotube atrophy and/or activity of downstream atrophy-associated proteins, such as the proteasome E3 ligases MAFbx and MURF1 are needed.

Summary

Skeletal muscle atrophy occurs as a result of many conditions and involves many molecular signaling pathways. Elevated intracellular Ca^{2+} is present in most of these atrophy states and is definitely implicated in disuse atrophy. Ca^{2+} is a potent stimulator of calpains, which exert considerable control over skeletal muscle atrophy by cleaving the intermediate filaments in the sarcomere to release the contractile proteins for degradation by the proteasome. Little is known about the regulation of calpains, but NO has been suggested as a calpain

inhibitor. If this is true in skeletal muscle, and NO does in fact inhibit calpain cleavage of intermediate filaments and subsequent proteasome action, then it could play a significant role in the prevention of muscle atrophy when Ca^{2+} is elevated.

CHAPTER 3
MATERIALS AND METHODS

Experimental Designs

An immortal cell line of rat skeletal muscle cells called L6 (ATCC, Manassas, VA) was used for all experiments. The L6 myogenic cell line was isolated originally by Yaffe from primary cultures of rat thigh muscle. These cells fuse in culture to differentiate into multinucleated myotubes and are a widely used model to study differentiated skeletal muscle cells. The L6 myogenic cell line was chosen in lieu of the C2C12 myogenic cell line produced in mouse muscle because, unlike C2C12 myotubes, L6 myotubes will not contract when exposed to a Ca^{2+} challenge.

Three experiments were performed in order to establish elevated intracellular Ca^{2+} levels induced by treatment with A23187 (Sigma, St. Louis, MO) as a dose-dependent model of skeletal muscle atrophy that stimulates calpain proteolysis of intermediate filaments and increases molecular markers of proteasome activity and to determine whether or not exogenous NO can attenuate these effects. Initial experiments exposed these cells to 30-60 minutes of A23187, while cells in subsequent experiments were pre-conditioned for 60 minutes (two hours total incubation) with PAPA-NO (Cayman Chemical, Ann Arbor, MI), an NO donor with a half-life of 15 minutes before treatment with A23187. Some cells were pre-conditioned with L-NMMA (Cayman Chemical), a blocker of endogenous NO release. Calpeptin (Calbiochem/EMD Chemicals, Gibbstown, NJ), a known inhibitor of calpain I and II, was administered to some groups in order to compare the effects of NO with the potent but specific effects of the inhibitor. In all of these experiements, whole cell lysate was harvested from all groups and used for Western blot analysis.

Two additional experiments were performed in order to test whether or not the model induced visible myotube atrophy, not simply cellular re-modeling, and also to test the effects of NO on potential myotube atrophy. In these experiments cells were exposed to different doses of A23187 for a longer time period (24-28 hours) in order to allow atrophy to occur. Some cells were also treated with DETA-NO (Cayman Chemical), an NO donor with a half-life of 20 hours. Visual images were taken for image analysis to determine changes in myotube size. Cells treated for 24 hours were also harvested and measured for total protein.

Experiment 1 Design - Aim 1, Hypothesis 1A (Figure 3-1)

Experiment 1 was used to test elevated intracellular Ca^{2+} induced by treatment with A23187 as a dose-dependent model of skeletal muscle atrophy stimulating calpain proteolysis of intermediate filaments and increasing proteasome activity. It was also used to determine the dose(s) of A23187 that would induce atrophy signals and that would be used in subsequent experiments. Previous studies administered doses ranging from 1 μM to 100 μM (19, 21). L6 myoblasts were cultured and differentiated into myotubes for four days before undergoing either 30- or 60-minute treatments with A23187. Groups 1-4 were treated for 30 minutes with the following doses of A23187 dissolved in DMSO: 0 μM (DMSO vehicle only), 1 μM, 10 μM, 20 μM. Groups 5-8 were incubated for 60 minutes with the same doses of A23187. For all groups n = 3. After the treatment period, cells were immediately lysed and harvested, and the whole cell lysate was prepared for Western blotting. Western blots were performed to measure cleaved and total talin, MAFbx, phospho-FOXO3a, and phopho- and total Akt.

Experiment 2 Design - Aim 1, Hypothesis 1B (Figure 3-2)

Experiment 2 was used to determine the effect of exogenous administration of NO on calpain proteoloysis and proteasome activity after 60 minutes of treatment with A23187. L6

myoblasts were cultured and differentiated into myotubes for four days before undergoing 60-minute treatments with A32187. Some groups were also pre-conditioned for 60 minutes prior to the treatment period with either PAPA-NO or L-NMMA dissolved in NaOH. For pre-conditioned groups, media was not changed between pre-conditioning and treatment, resulting in two hours of total incubation time. Groups 1-3 received no A23187. Group 1 was incubated with only the DMSO vehicle, while groups 2 and 3 were pre-conditioned with PAPA-NO as follows: 1 μM (group 2), 10 μM PAPA-NO (group 3). Groups 4-7 were treated with 10 μM A23187. Group 4 received no pre-conditioning, while groups 5, 6, and 7 were pre-conditioned as follows: 1 μM PAPA-NO (group 5), 10 μM PAPA-NO (group 6), 5 mM L-NMMA (group 7). Groups 8-11 were treated with 20 μM A23187. Group 8 received no pre-conditioning, while groups 9, 10, and 11 were pre-conditioned as follows: 1 μM PAPA-NO (group 9), 10 μM PAPA-NO (group 10), 5 mM L-NMMA (group 11). For all groups n = 6. After the treatment period, cells were immediately lysed and harvested, and the whole cell lysate was prepared for Western blotting. Total protein was measured, and Western blots were performed to probe for cleaved and total talin, MAFbx, phospho-FOXO3a, and phopho- and total Akt.

Experiment 3 Design – Aim 1, Hypothesis 1B (Figure 3-3)

Experiment 3 was used to compare the effects of NO on calpain proteoloysis and proteasome activity with those of calpeptin, a known calpain inhibitor, after 60 minutes of treatment with A23187. L6 myoblasts were cultured and differentiated into myotubes for four days before undergoing 60-minute treatments with A32187. Some groups were also pre-conditioned for 60 minutes prior to the treatment period with either PAPA-NO dissolved in NaOH and/or calpeptin dissolved in DMSO as described above. Group 1 received no treatments (DMSO vehicle only). Groups 2-7 were treated with 20 μM A23187. Group 2 received no

pre-conditioning, while groups 3-7 were pre-conditioned as follows: 1 μM NO (group 3), 10 μM NO (group 4), 100 μM calpeptin (group 5), 1 μM NO + 100 μM calpeptin (group 6), 10 μM NO + 100 μM calpeptin (group 7). For all groups n=6. After the treatment period, cells were immediately lysed and harvested, and the whole cell lysate was prepared for Western blotting. Western blots were performed to probe for cleaved and total talin, MAFbx, phospho-FOXO3a, and phopho- and total Akt.

Experiment 4 Design – Aim 2, Hypothesis 2A (Figure 3-4)

Experiment 4 was used to test if elevated intracellular Ca^{2+} by treatment with A23187 induces visible myotube atrophy (loss of size and/or total protein) after 24-48 hours. L6 myoblasts were cultured and differentiated into myotubes for four days before being treated for either 24 or 48 hours with A23187. Groups 1-6 were treated for 24 hours with the following doses: 0 μM (DMSO only), 0.4 μM, 1 μM, 5 μM, 10 μM, 20 μM. Groups 7-12 were treated for 48 hours with the same doses. For all groups n = 3. For cells undergoing the 24-hour treatment, visual images were captured with a light microscope and analyzed immediately following treatment. These cells were then harvested and measured for total protein. Cells undergoing the 48-hour treatment were washed with PBS immediately following treatment and fixed with paraformaldehyde solution for visual analysis with a light microscope.

Experiment 5 Design – Aim 2, Hypothesis 2B (Figure 3-5)

Experiment 5 was used to test the effects of NO myotube atrophy following 24-48 hours of treatment with A23187. L6 myoblasts were cultured and differentiated into myotubes for four days before being treated for either 24 or 48 hours with A23187. Some groups were also treated with DETA-NO dissolved in NaOH. All of the following groups were tested at both 24 hours and 48 hours. Groups 1-3 received no A23187. Group 1 received no treatments (DMSO vehicle

only), while groups 2 and 3 were treated with either 1 μM DETA-NO (group 2) or 10 μM DETA-NO (group 3). Groups 4-6 were treated with 10 μM A23187. Group 4 received no DETA-NO, while groups 5 and 6 were pre-conditioned with either 1 μM DETA-NO (group 5) or 10 μM DETA-NO (group 6). Groups 7-9 were treated with 20 μM A23187. Group 7 received no DETA-NO, while groups 8 and 9 were pre-conditioned with either 1 μM DETA-NO (group 8) or 10 μM DETA-NO (group 9). For all groups n = 3. For cells undergoing the 24-hour treatment, visual images were captured with a light microscope and analyzed immediately following treatment. These cells were then harvested and measured for total protein. Cells undergoing the 48-hour treatment were washed with PBS immediately following treatment and fixed with paraformaldehyde solution for visual analysis with a light microscope.

General Methods

Myogenic Culture

Myoblasts derived from L6 cells (ATCC, Manassas, VA) were cultured on 100 mm dishes in Dulbecoo's Modified Eagle's Medium (DMEM) (Mediatech, Herndon, VA) supplemented with 10% fetal bovine serum (FBS), 1% penicillin/streptomycin, and 0.1% funzigone at 37°C in the presence of 5% CO_2 until 60-70% confluence was reached as visualized by light microscopy. The cultures were then trypsinized and re-plated at equal density to 6-well plates for differentiation and treatment. Once the plate cultures reached 70-80% confluency, myotube differentiation was initiated by switching to DMEM supplemented with 2% horse serum, 1% penicillin/streptomycin, and 0.1% fungizone.

Image Analysis

Three to six digital images per culture were captured using a Zeiss microscope. The images were analyzed for myotube length, diameter and area using ImageJ imaging software (NIH).

Whole Cell Lysate

Cells were harvested in ice-cold non-denaturing lysis (NDL) buffer containing 30 mM Tris-HCL (pH 7.5), 0.7% Triton-X, 150 mM NaCl, 3.5 mM EDTA, 10 mg/ml NaN_3, 1 μM Na_3VO_4, 0.05% vol/vol protease inhibitors and 0.5% vol/vol phosphatase inhibitors (Sigma, St. Louis, MO). Lysates were then centrifuged at 4°C for 10 minutes at 1000 x g.

Western Blot Analysis

Protein concentrations were measured using the D_C Protein Assay Kit (Bio-Rad Laboratories, Richmond, CA). Aliquots of whole cell lysate were run on SDS-PAGE gels, and proteins were transferred to either PVDF membranes (for phospho-FOXO3a) or nitrocellulose (NC) membranes (all others). Protein transfer was confirmed by Ponceau staining. Membranes were then blocked with either 5% milk + 0.1% Tween-20 in TBS (PVDF) or Odyssey blocking buffer (NC) (LI-COR Biosciences, Lincoln, NE) for one hour. The membranes were then washed three times with 0.1% Tween-20 in TBS and incubated at 4°C overnight in primary antibodies diluted with either 5% BSA + 0.1% Tween-20 in TBS (PVDF) or Odyssey blocking buffer (NC). Primary antibodies were applied for: talin (Sigma, St. Louis, MO), MAFbx (Santa Cruz, Santa Cruz, CA), phospho-FOXO3a (Cell Signaling, Danvers, MA), phospho-Akt (Santa Cruz, Santa Cruz, CA), total Akt (Santa Cruz, Santa Cruz, CA). Beta-actin (Abcam; Cambridge, MA) was used as a loading control. After overnight incubation, membranes were washed again with 0.1% Tween-20 in TBS three times and then incubated for 35 minutes in secondary antibody diluted with either 0.1% Tween-20 in TBS (PVDF) or Odyssey blocking buffer (NC). The secondary antibodies were IR Dye conjugated secondaries detectable at wavelengths of 680 or 800 nm (LI-COR) and non-fluorescent anti-rabbit IgG. Membranes were washed three times with 0.1% Tween-20 in TBS and then once with either EDL-plus (PVDF) or

TBS (NC) before being scanned and detected using either Kodak film processing (PVDF) or the Odyssey infrared imaging system (NC) (LI-COR).

Statistical Analysis

Group sample size was determined with power analysis of our preliminary data. Comparisons between groups were made by a 2-way or 3-way full-factorial ANOVA, and when appropriate, Tukey's HSD test was performed post-hoc. Significance was established at $p < 0.05$.

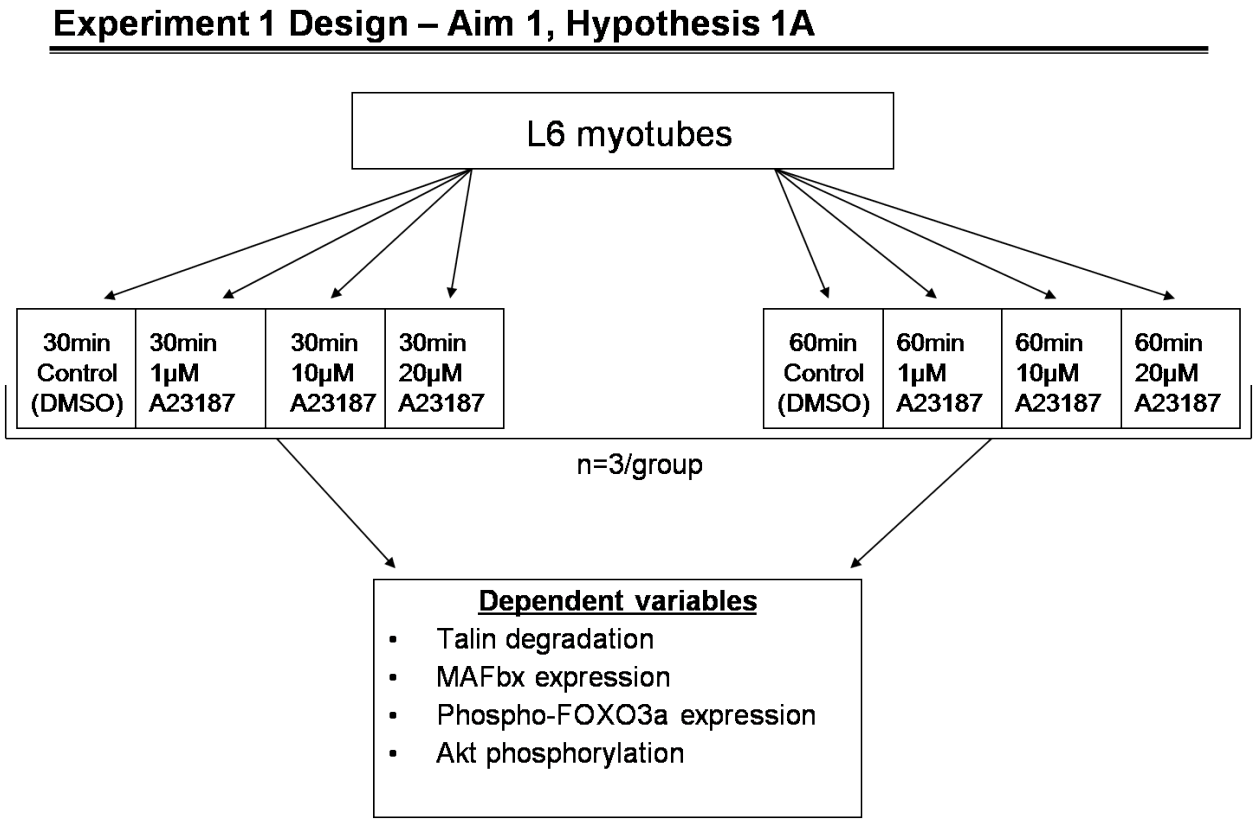

Figure 3-1. Experiment 1 design – Aim 1, Hypothesis 1A. The purpose was to test elevated intracellular Ca2+ induced by treatment with A23187 as a dose-dependent model of skeletal muscle atrophy stimulating calpain proteolysis of intermediate filaments and increasing proteasome activity.

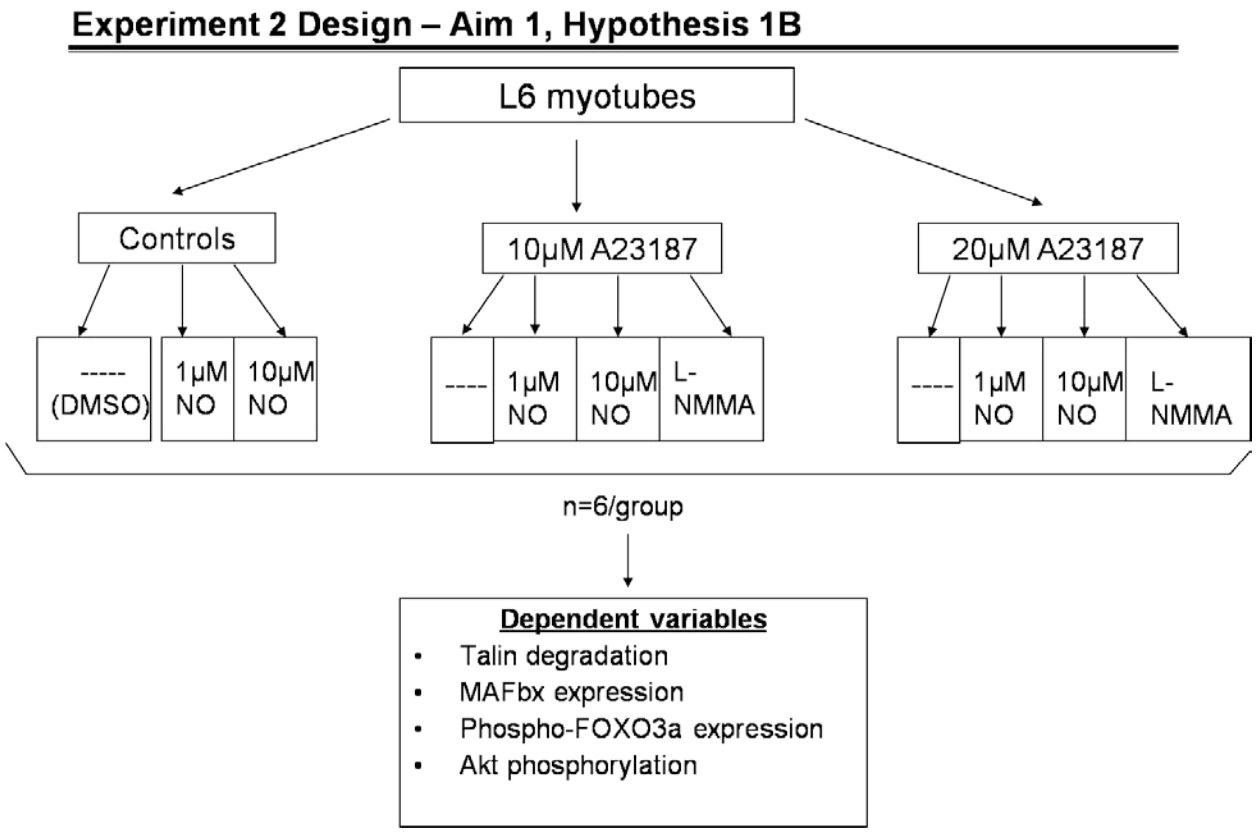

Figure 3-2. Experiment 2 design – Aim 1, Hypothesis 1B. Purpose was to determine the effect of exogenous administration of NO on calpain proteoloysis and proteasome activity after 60 minutes of treatment with A23187.

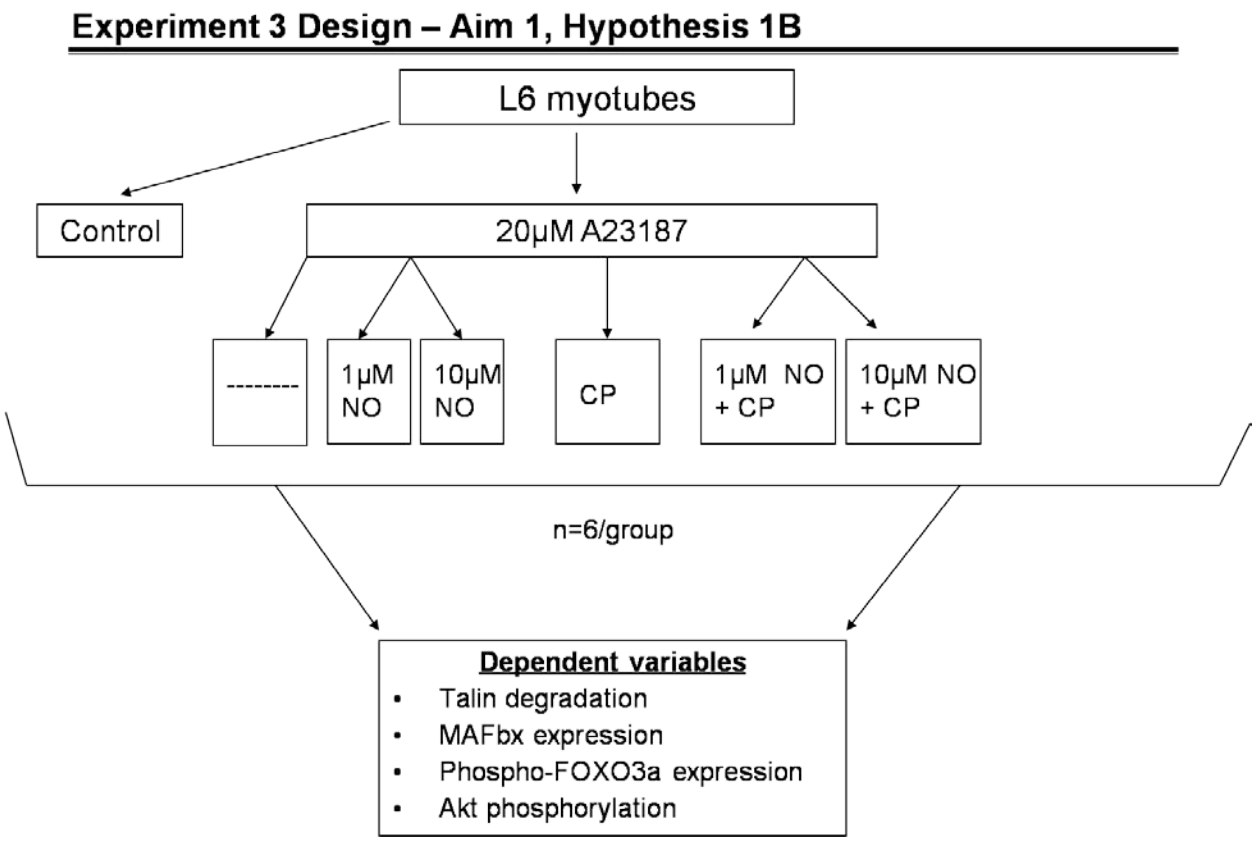

Figure 3-3. Experiment 3 design – Aim 1, Hypothesis 1B. Purpose was to compare the effects of NO on calpain proteolysis and proteasome activity with those of calpeptin, a known calpain inhibitor, after 60 minutes of treatment with A23187.

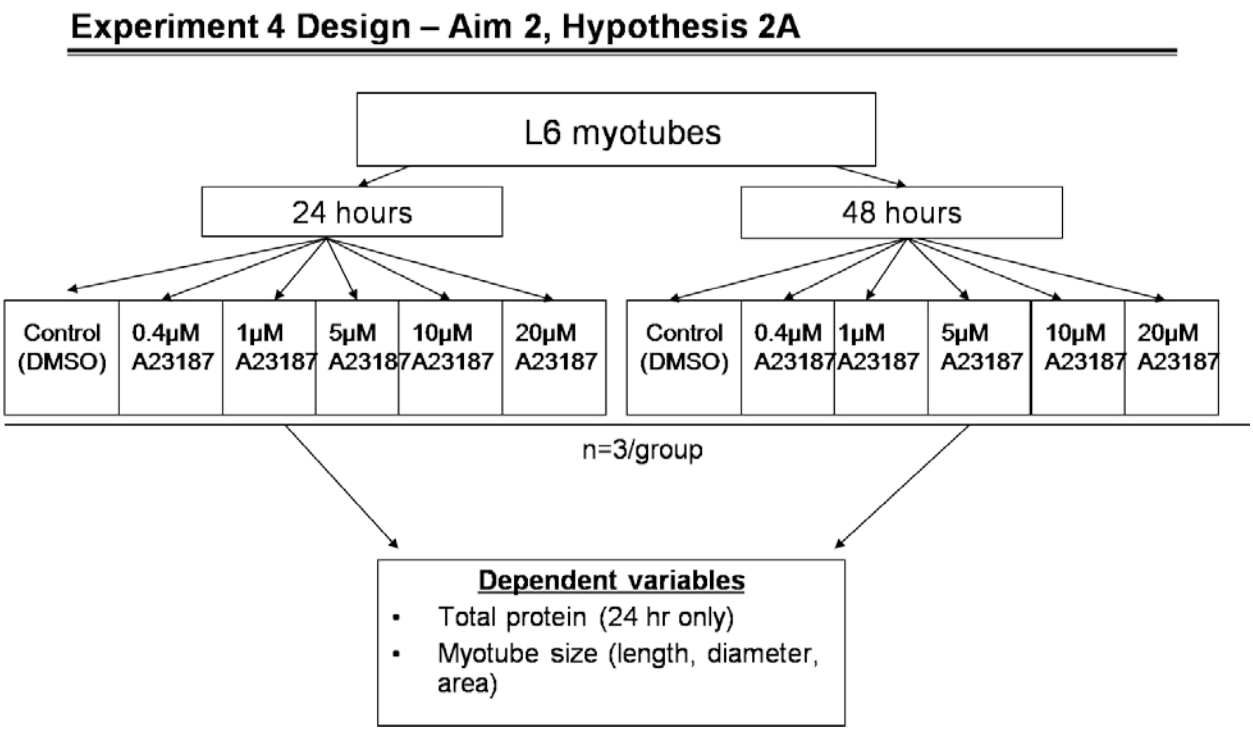

Figure 3-4. Experiment 4 design – Aim 2, Hypothesis 2A. Purpose was to test if elevated intracellular Ca^{2+} by treatment with A23187 induces visible myotube atrophy after 24-28 hours.

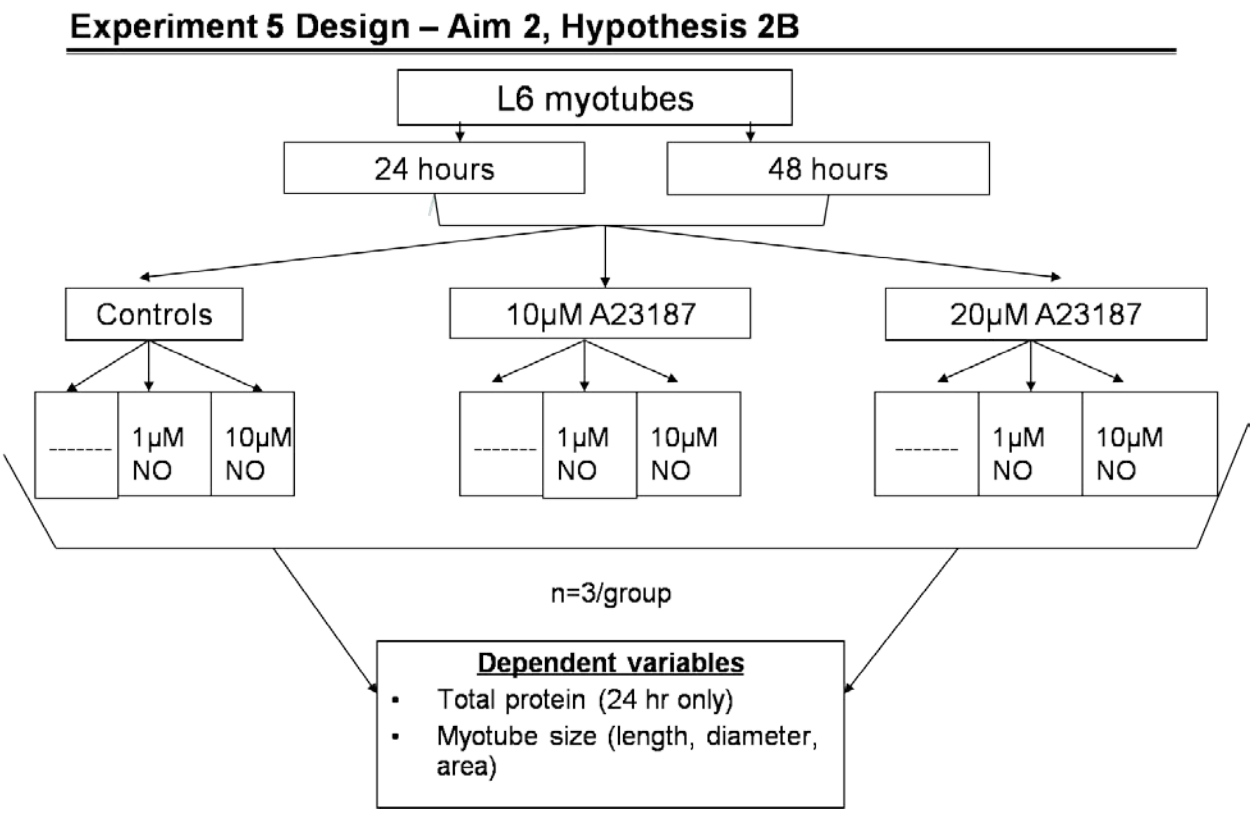

Figure 3-5. Experiment 5 design - Aim 2, Hypothesis 2B. Purpose was test the effects of NO myotube atrophy following 24-48 hours of treatment with A23187.

CHAPTER 4
RESULTS

Effects of Treatment with A23187 and NO on Molecular Markers

Specific aim 1 was to test that elevated intracellular Ca^{2+} levels induced by treatment with A23187 is a dose-dependent model of skeletal muscle atrophy stimulating calpain proteolysis of intermediate filaments and increasing molecular markers of proteasome activity and to determine whether or not exogenous NO can attenuate these effects.

Talin

In experiment 1, the ratio of cleaved to total talin increased significantly after 60 minutes of treatment with 20 µM A23187 (Figures 4-1). And, although increased talin cleavage at other doses did not meet statistical significance with n=3 and $p < 0.05$, there was an apparent trend toward progressively more talin cleavage with increasing dose of A23187 (Figure 4-1). No significant changes were seen in talin cleavage after 30 minutes of treatment. In experiment 2, talin cleavage significantly increased after 60 minutes of treatment with 10 µM A23187 and with 10 µM A23187 + L-NMMA, a blocker of endogenous NO release (Figure 4-2). Pre-conditioning with both 1 µM PAPA-NO and 10 µM PAPA-NO appeared to attenuate the increase in talin cleavage after treatment with 10 µM A23187, as cleavage levels were reduced to near control (not statistically different from control at $p < 0.05$) (Figure 4-2). Talin cleavage also significantly increased after treatment with 20 µM A23187 + 1 µM PAPA-NO and with 20 µM A23187 + L-NMMA (Figure 4-2). However, pre-conditioning with 10 µM PAPA-NO appeared to attenuate the increase in talin cleavage after treatment with 20 µM A23187, as the cleavage level was similar to control and significantly lower than with 20 µM A23187 + 1 µM PAPA-NO and with 20 µM A23187 + L-NMMA (Figure 4-2). Talin cleavage was significantly reduced by

treatment with calpeptin, a specific calpain inhibitor, but concurrent treatment with PAPA-NO did not provide additional protection (Figure 4-3).

Akt

In experiment 1, the ratio of phosphorylated (active) Akt to total Akt protein appeared to increase after 60 minutes of treatment with 10 µM and 20 µM doses of A23187, but the increases did not meet statistical significance with n=3 and $p < 0.05$ (Figure 4-4). No changes were seen after 30 minutes of treatment with A23187 at any dose (Figure 4-4). In experiment 2, the ratio of phosphorylated (active) Akt to total Akt protein significantly increased after 60 minutes of treatment with 10 µM A23187 + 1 µM PAPA-NO, 10 µM A23187 + 10 µM PAPA-NO, and 10 µM A23187 + L-NMMA, but there were no differences among these groups (Figure 4-5). Groups treated with 20 µM A23187 showed no significant differences in Akt ratio (Figure 4-5). The ratio of phosphorylated Akt to total Akt was not altered with calpeptin treatment for any treatment group (Figure 4-6).

FOXO3a

In experiment 1, phosphorylated (inactive, cytosolic) FOXO3a protein expression did not significantly change after either 30 or 60 minutes of treatment with various doses of A23187 (Figure 4-7). However, treatment with 20 µM A23187 for 60 minutes did appear to slightly decrease the expression of phospho-FOXO3a (Figure 4-7). In experiment 2, treatment with 10 µM A23187 alone and with 10 µM A23187 + 1 µM PAPA-NO significantly increased phospho-FOXO3a expression, but no other treatment groups showed significant differences (Figure 4-8). Treatment with calpeptin did not affect phospho-FOXO3a expression except when combined with 10 µM PAPA-NO; calpeptin + 10 µM PAPA-NO resulted in significantly lower expression of phospho-FOXO3a after 60 minutes of treatment with 20 µM A23187 (Figure 4-9).

MAFbx

In experiment 1, MAFbx protein expression did not significantly change after either 30 or 60 minutes of treatment with various doses of A23187 (Figure 4-10). In experiment 2, MAFbx protein expression did not significantly change with any combination of 10 µM A23187 and PAPA-NO (Figure 4-11). Treatment with 20 µM A23187, 20 µM A23187 + 1 µM PAPA-NO, and 20 µM A23187 + 10 µM PAPA-NO significantly decreased MAFbx expression as compared to control groups, but there were no differences among these groups (Figure 4-11). Treatment with either dose of A23187 + L-NMMA appeared to possibly increase MAFbx expression as compared to A23187 alone, but these differences did not reach statistical significance at $p < 0.05$ (Figure 4-11). MAFbx protein expression was not altered with calpeptin treatment for any treatment group (Figure 4-12).

Effects of A23187 Treatment and NO on Myotube Atrophy

Specific aim 2 was to test if elevated intracellular Ca^{2+} by treatment with A23187 induces myotube atrophy (loss of size and/or total protein) and whether or not exogenous NO administration results in decreased atrophy.

Protein Degradation

Muscle protein degradation increased in L6 myotubes undergoing 24 hours of treatment with A23187 (Figure 4-13). Cells exposed to 5, 10, and 20 µM A23187 exhibited significantly more protein degradation than control. Although the differences among these three groups did not meet statistical significance with $n=3$ and $p < 0.05$, there was an apparent trend toward progressively greater protein degradation with increasing doses of A23187. Doses of 50 µM and 100 µM were also tested in preliminary experiments, but cell viability was much poorer at these high levels, so the doses were discontinued and protein was not measured.

When cells were treated with A23187 with and without DETA-NO for 24 hours, there were no significant differences in protein degradation between groups treated with NO and those treated without NO (Figure 4-14). Cells treated with A23187 had significantly less protein than cells without A23187, as was observed in the previous experiment. A23187 had a significant main effect at $p < 0.0001$, but there was no significant effect of NO on protein degradation.

Myotube Image Analysis

Visual images were captured after 24 and 48 hours of treatment with A23187 (Figure 4-15), and myotube diameter, length, and area were measured. Preliminary data images from groups treated with 50 µM A23187 were analyzed for additional comparison. After 24 hours, myotube diameter was significantly decreased with 10 µM A23187 treatment (Figure 4-16A), myotube length was significantly decreased with 50 µM A23187 treatment (Figure 4-16B), and myotube area was significantly decreased with 50 µM A23187 treatment (Figure 4-16C). No other significant differences in myotube size were observed after 24 hours. After 48 hours, no differences in myotube diameter were observed (Figure 4-16A), but myotube length significantly decreased with both 10 µM and 50 µM A23187 as compared to both untreated control and with 24 hours with 1 µM A23187 (Figure 4-16B). Also after 48 hours, myotube area was significantly decreased with 10 µM, 20 µM, and 50 µM A23187 as compared to both untreated control and with 24 hours with 1 µM A23187 (Figure 4-16C).

Visual images were again captured after 24 hours of treatment with A23187 with and without DETA-NO (Figure 4-17). Image capture was stopped and analysis was omitted for cells treated for 48 hours due to myotube deterioration. Images of cells treated for 24 hours were analyzed; myotube diameter, length, and area were measured (Figures 4-18, 4-19, 4-20). Myotubes treated with 1 µM DETA-NO alone had siginificantly increased diameter, length, and area when compared to untreated cells (Figures 4-18, 4-19, 4-20).

Treatment with either 10 µM A23187 or 20 µM A23187 alone significantly decreased myotube diameter, while concurrent NO treatment significantly attenuated the decreases (Figure 4-18). For cells treated with 10 µM A23187, those without DETA-NO had significantly decreased diameter as compared to untreated controls. However, concurrent treatment with either 1 µM DETA-NO or 10 µM DETA-NO resulted in myotube diameter similar to that of untreated control cells. Additionally, concurrent treatment with 10 µM DETA-NO significantly increased myotube diameter as compared to 10 µM A23187 alone. For cells treated with 20 µM A23187, those without DETA-NO had significantly decreased diameter as compared to untreated controls. However, concurrent treatment with either 1 µM DETA-NO or 10 µM DETA-NO resulted in significantly greater myotube diameter than the lower dose 10 µM A23187 alone, indicating partial protection of myotube diameter. Concurrent treatment with 1 µM DETA-NO also significantly increased myotube diameter as compared to 20 µM A23187 alone.

Treatment with either 10 µM or 20 µM A23187 alone significantly decreased myotube length, but NO had no effect on the decreases in length for any dose combination (Figure 4-19). There was a significant main effect for DETA-NO treatment, but increased length was only observed for 1 µM DETA-NO alone. DETA-NO failed to attenuate the decreased length seen in groups treated with A23187.

Treatment with either 10 µM or 20 µM A23187 alone also significantly decreased myotube area, but concurrent NO treatment did attenuate the loss of myotube area for cells treated at the lower dose of 10 µM A23187 (Figure 4-20). For cells treated with 10 µM A23187, those without DETA-NO and those with 1 µM DETA-NO had significantly decreased myotube area as compared to untreated controls. However, cells concurrently treated with 10 µM DETA-NO had myotube area similar to untreated controls and significantly greater than those

with 10 μM A23187 alone. For cells treated with 20 μM A23187, neither dose of DETA-NO significantly changed the myotube area.

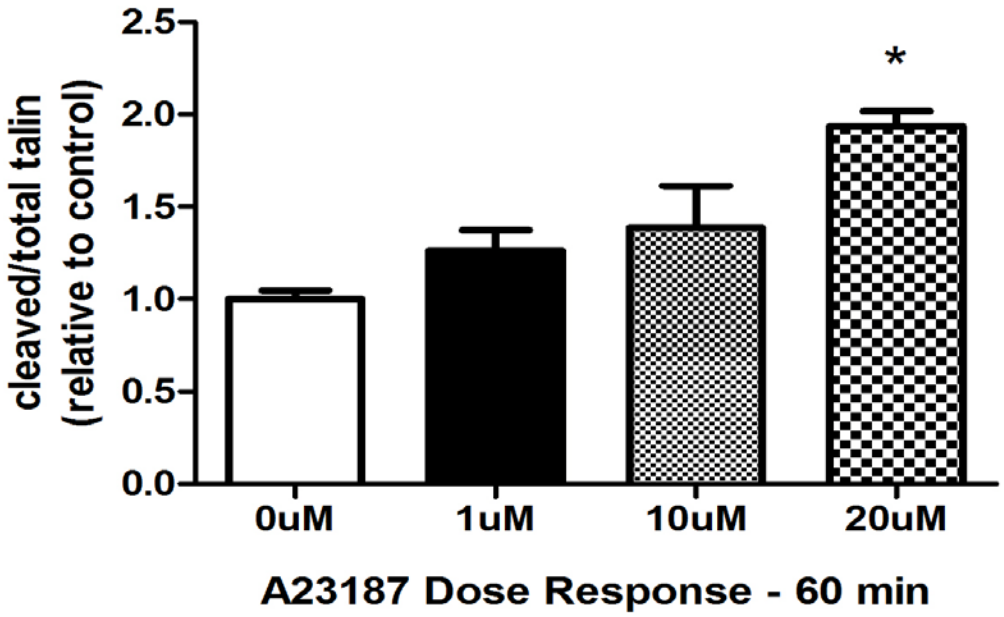

Figure 4-1. Talin cleavage in L6 myotubes after 60 minutes of treatment with A23187. Values represent the mean ± SEM (n=3). *Significantly different from control ($p < 0.05$).

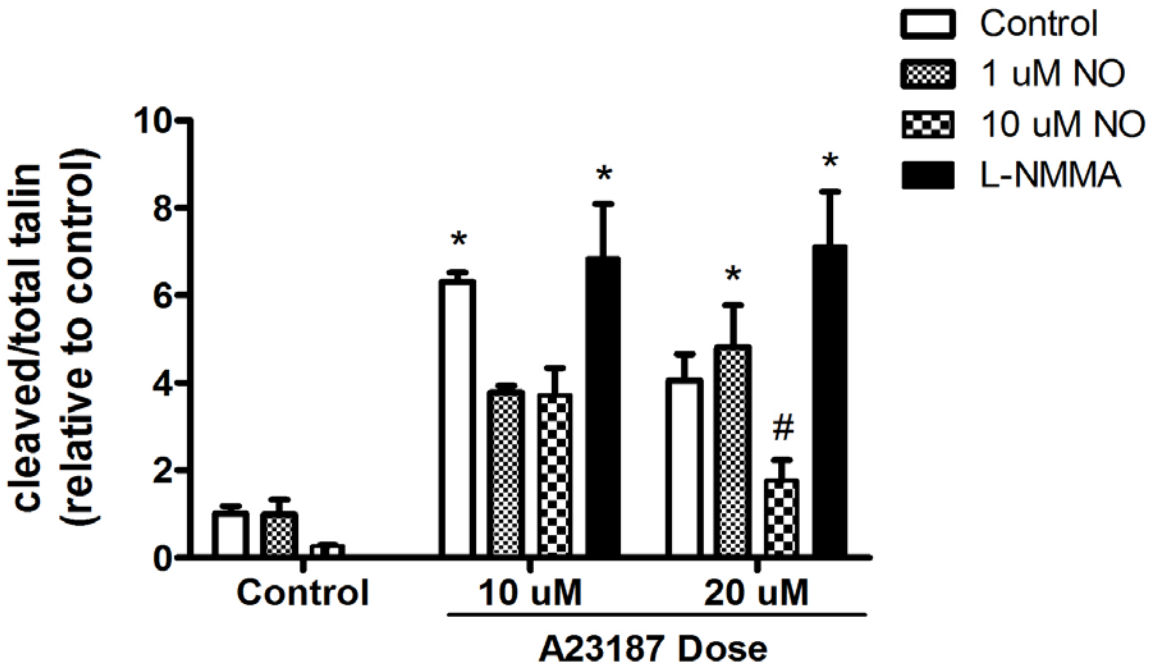

Figure 4-2. Talin cleavage in L6 myotubes after 60 minutes of treatment with A23187 and/or PAPA-NO or L-NMMA pre-conditioning. Values represent the mean ± SEM (n=3). *Significantly different from control ($p < 0.05$). #Significantly different from 20 µM A23187 + 1 µM NO and 20 µM A23187 + L-NMMA ($p < 0.05$).

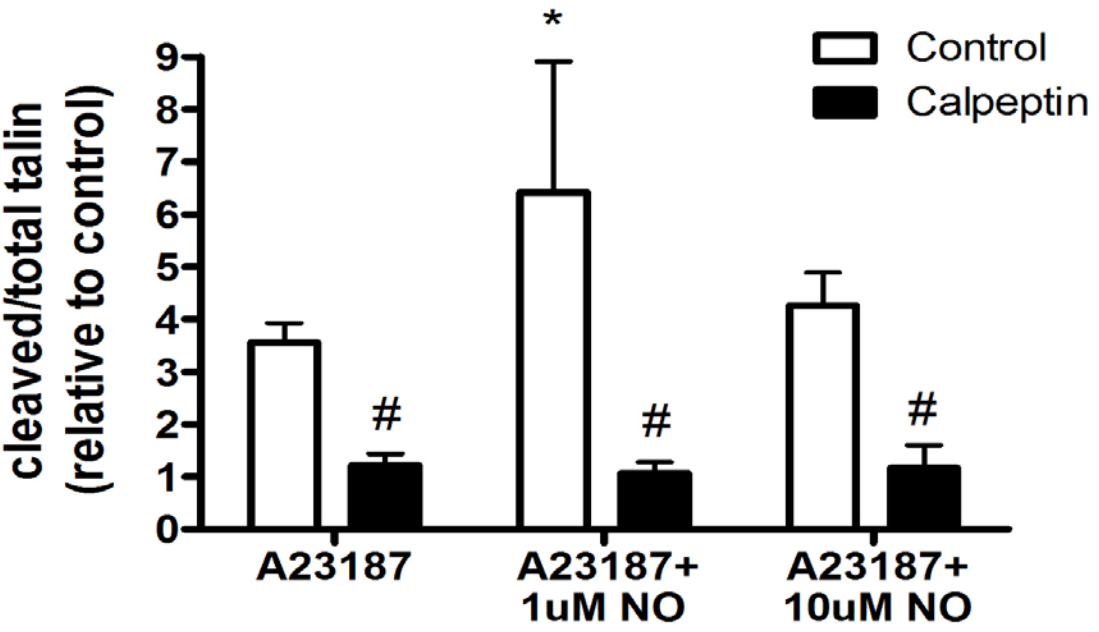

Figure 4-3. Talin cleavage in L6 myotubes after 60 minutes of treatment with 20 µM A23187 and/or PAPA-NO pre-conditioning with and without calpeptin. Values represent the mean ± SEM (n=4). *Significantly different from 20 µM A23187 control ($p < 0.05$). #Significantly different from same treatment without calpeptin ($p < 0.05$).

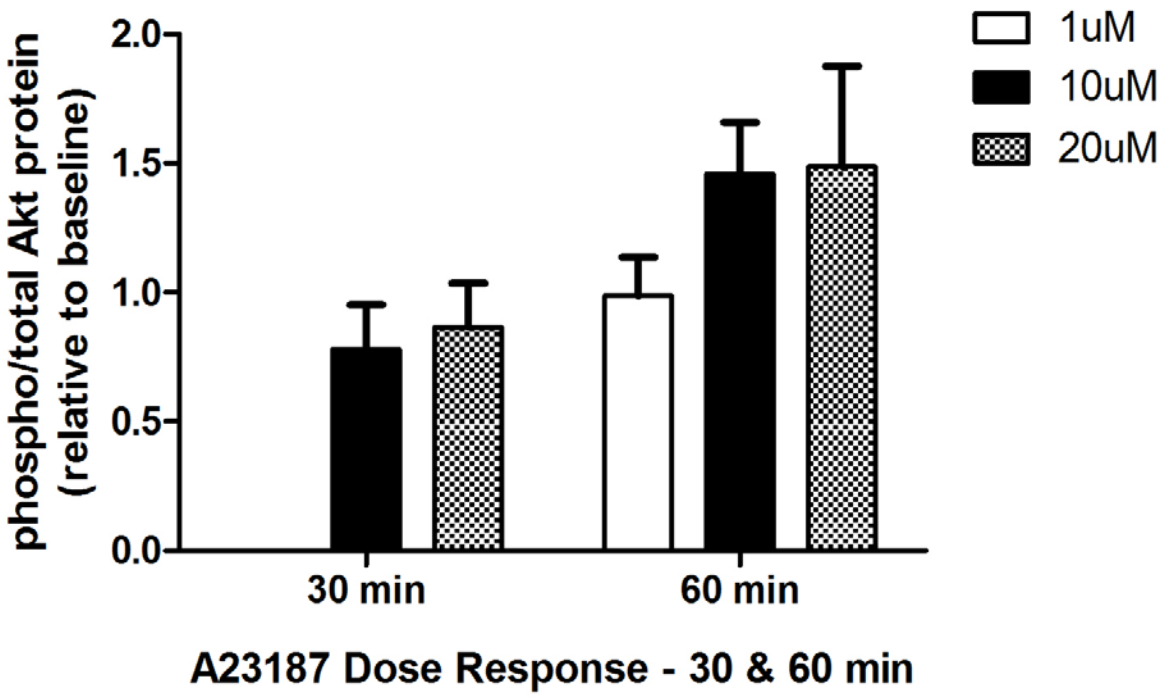

Figure 4-4. Phopho/Total Akt protein expression in L6 myotubes after 30 or 60 minutes of treatment with A23187. Values represent the mean ± SEM (n=3).

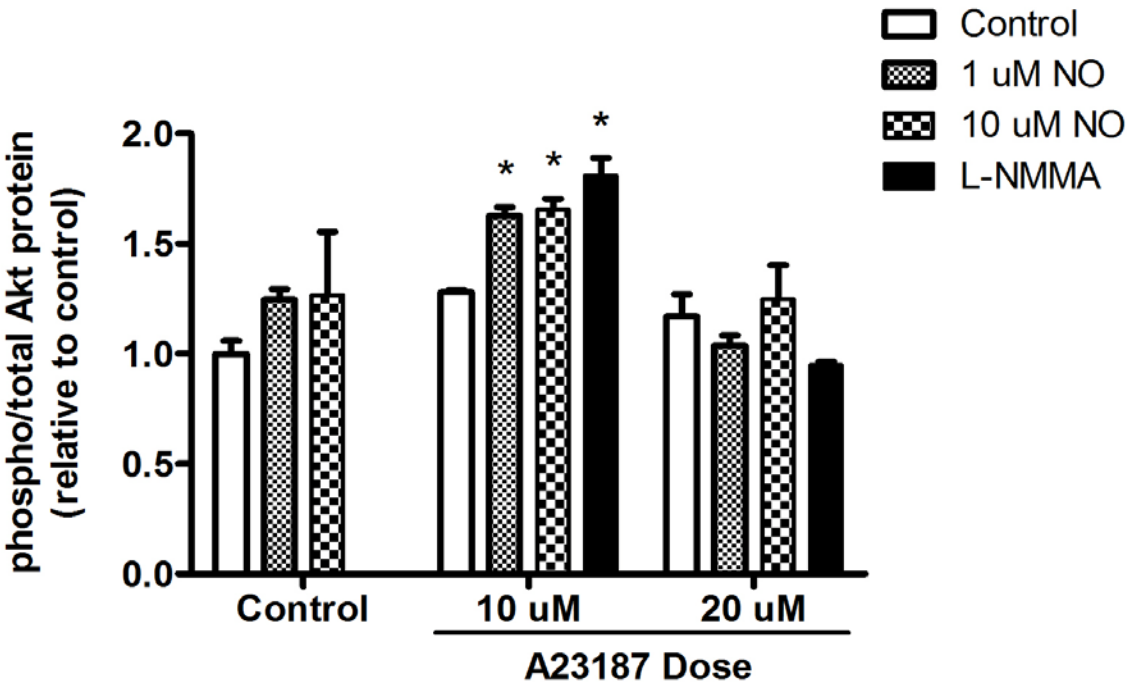

Figure 4-5. Phospho/Total Akt protein expression in L6 myotubes after 60 minutes of treatment with A23187 and/or PAPA-NO or L-NMMA pre-conditioning. Values represent the mean ± SEM (n=3). *Significantly from control groups ($p < 0.05$).

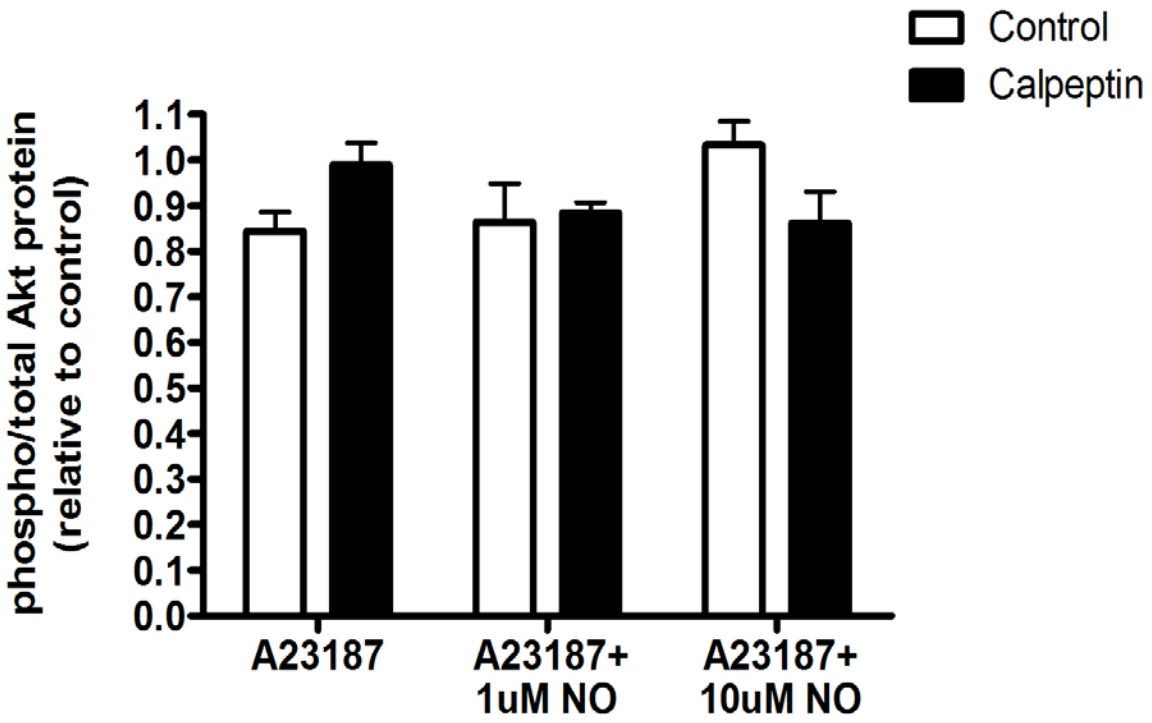

Figure 4-6. Phospho/Total Akt protein expression in L6 myotubes after 60 minutes of treatment with 20 µM A23187 and/or PAPA-NO pre-conditioning with and without calpeptin. Values represent the mean ± SEM (n=4).

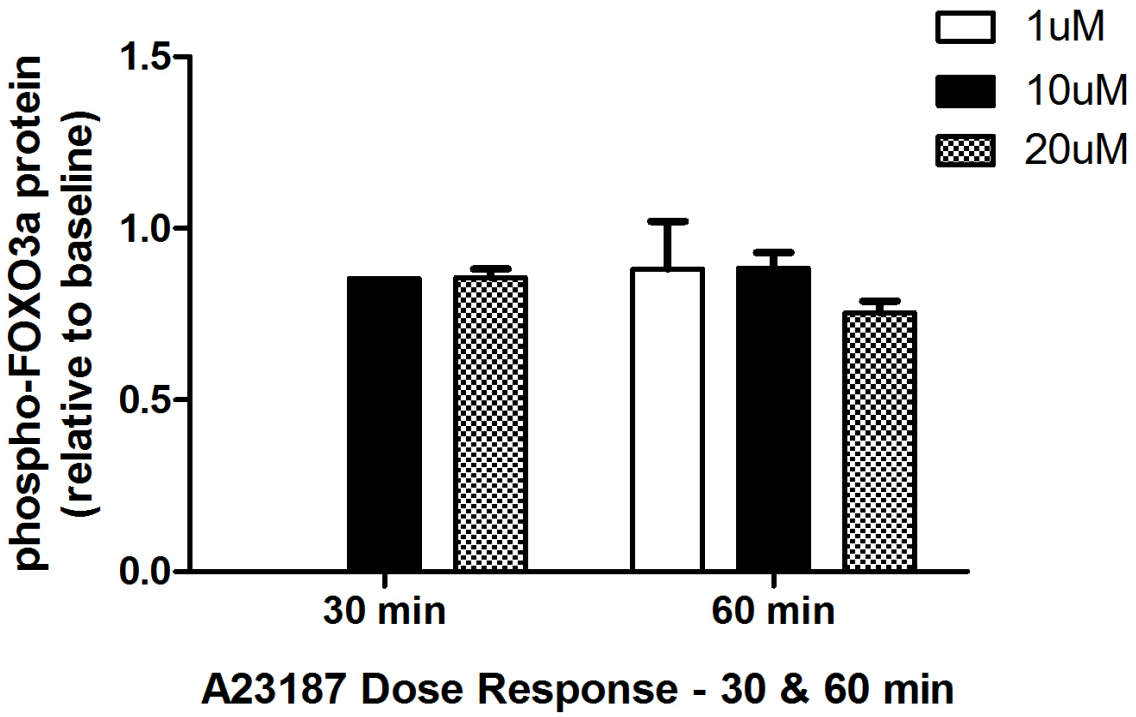

Figure 4-7. Phospho-FOXO3a protein expression in L6 myotubes after 30 or 60 minutes of treatment with A23187. Values represent the mean ± SEM (n=3).

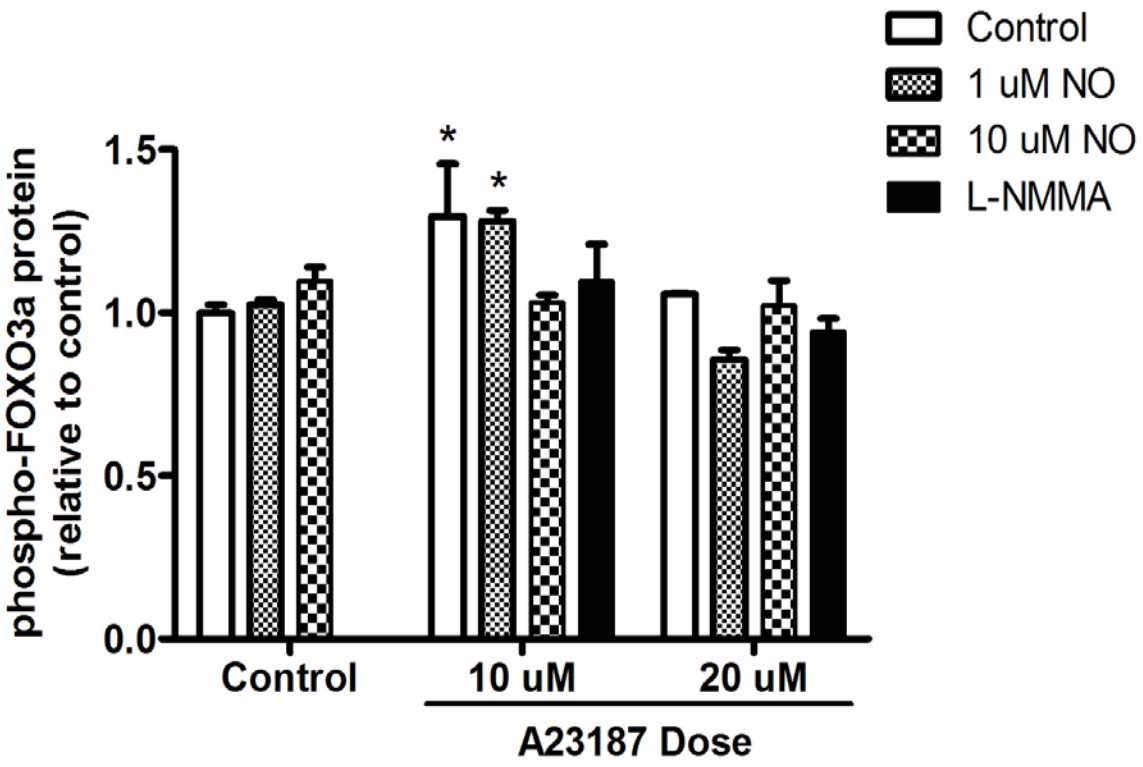

Figure 4-8. Phospho-FOXO3a protein expression in L6 myotubes after 60 minutes of treatment with A23187 and/or PAPA-NO or L-NMMA pre-conditioning. Values represent the mean ± SEM (n=3). *Significantly different from control groups ($p < 0.05$).

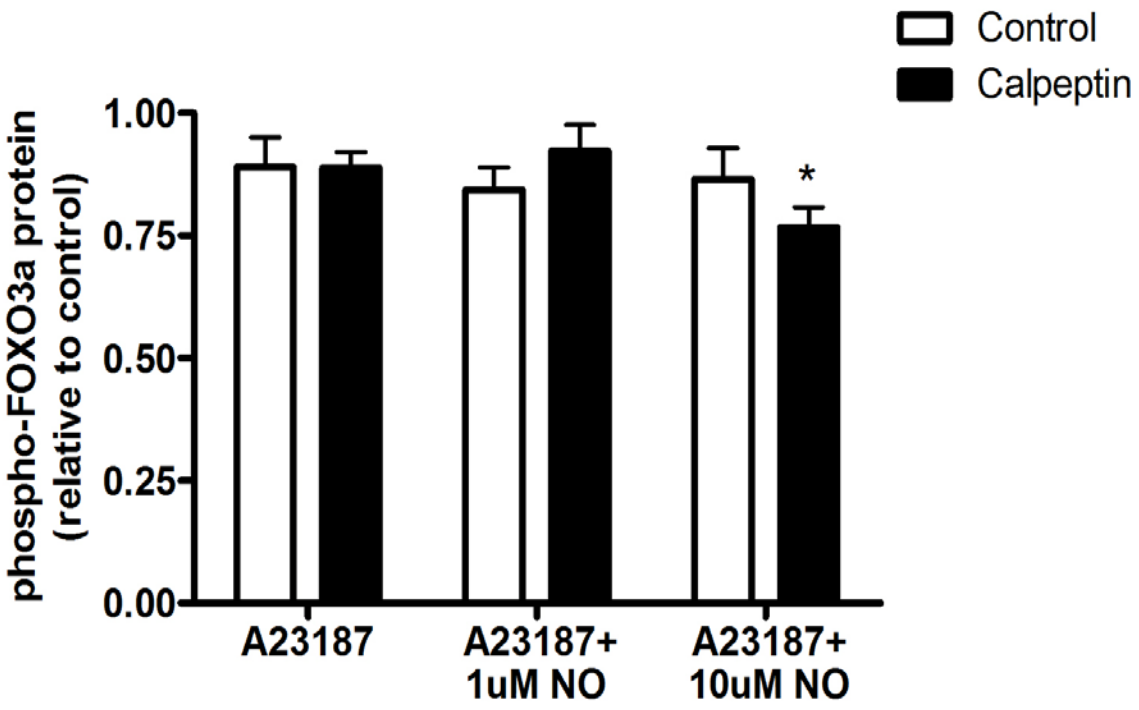

Figure 4-9. Phospho-FOXO3a protein expression in L6 myotubes after 60 minutes of treatment with 20 µM A23187 and/or PAPA-NO pre-conditioning with and without calpeptin. Values represent the mean ± SEM (n=4). *Significantly different from control ($p < 0.05$).

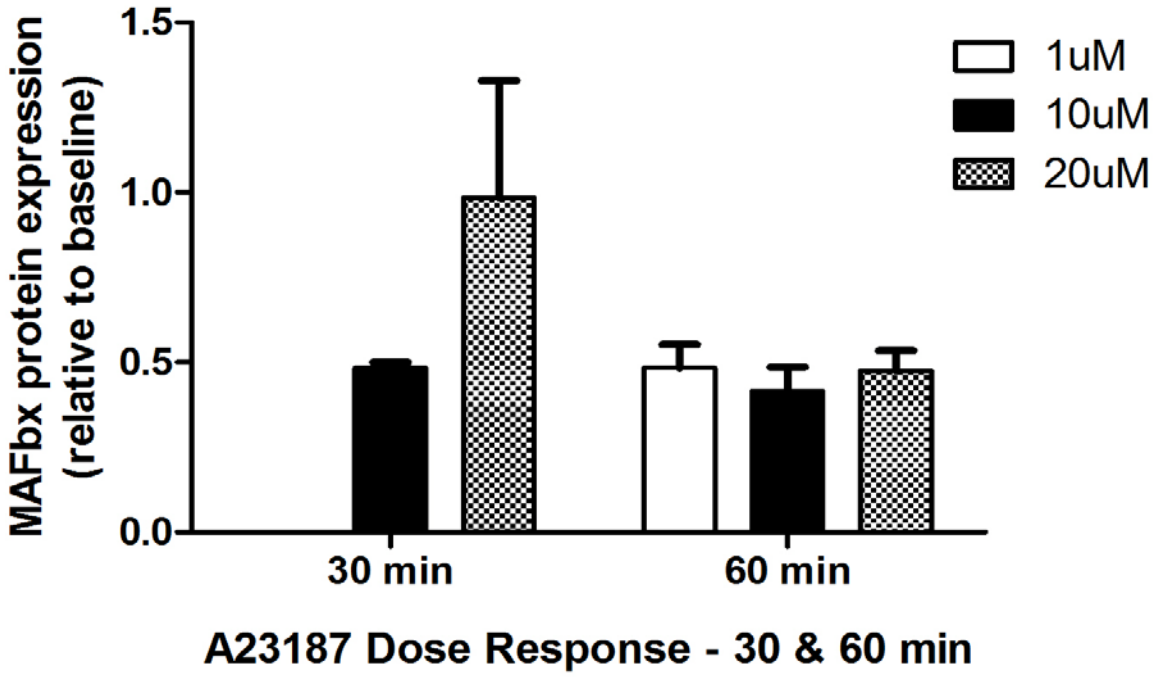

Figure 4-10. MAFbx protein expression in L6 myotubes after 30 or 60 minutes of treatment with A23187. Values represent the mean ± SEM (n=3).

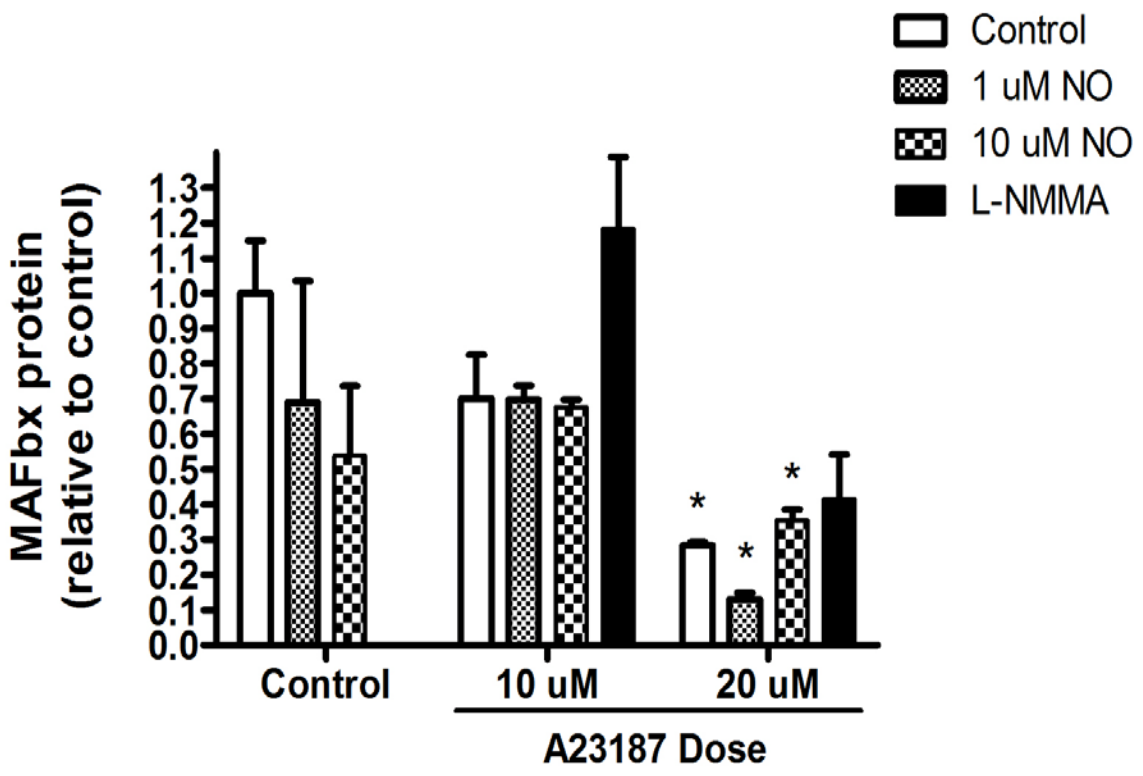

Figure 4-11. MAFbx protein expression in L6 myotubes after 60 minutes of treatment with A23187 and/or PAPA-NO or L-NMMA pre-conditioning. Values represent the mean ± SEM (n=3). *Significantly different from control groups ($p < 0.05$).

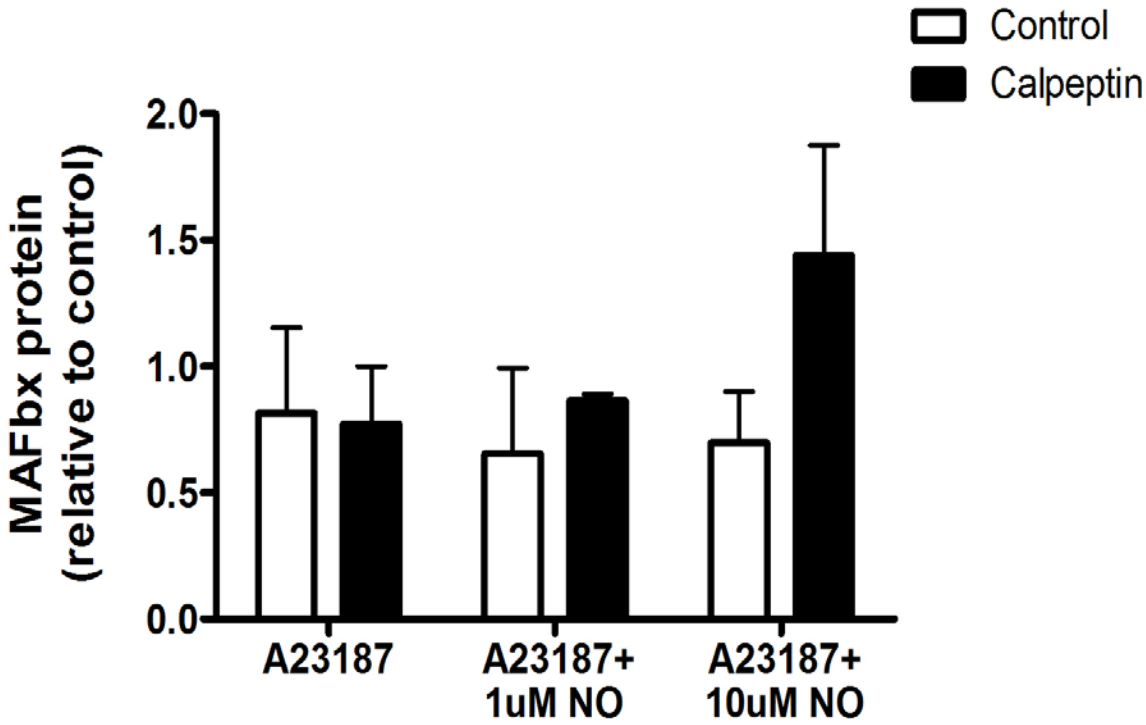

Figure 4-12. MAFbx protein expression in L6 myotubes after 60 minutes of treatment with 20 µM A23187 and/or PAPA-NO pre-conditioning with and without calpeptin. Values represent the mean ± SEM (n=4).

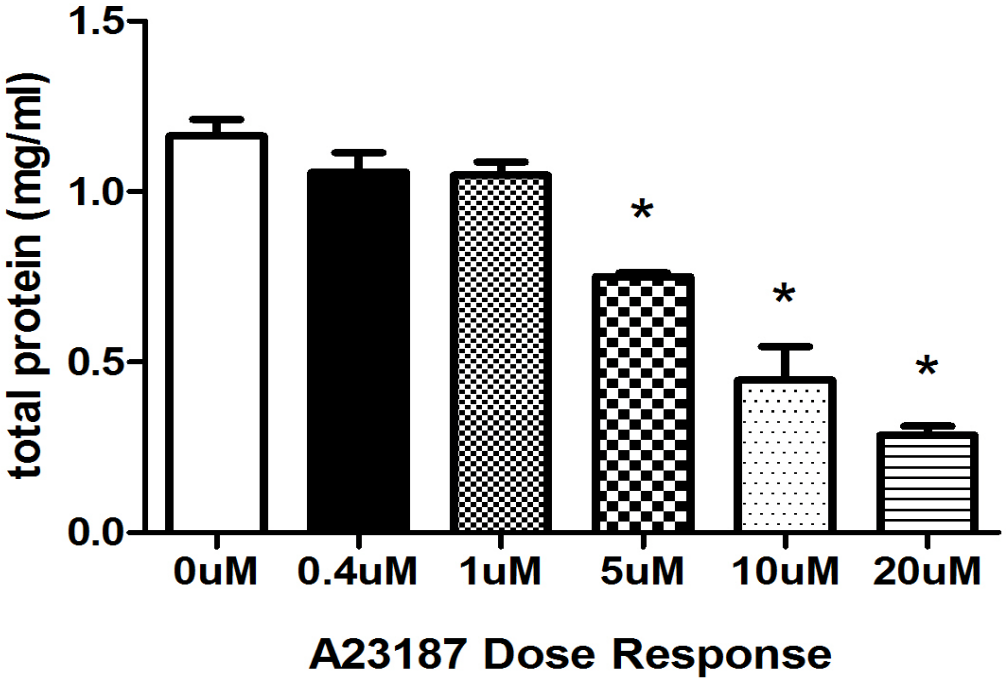

Figure 4-13. Total protein concentrations for L6 myotubes after 24 hours treatment with A23187. Values represent the mean ± SEM (n=3). *Significantly different from control ($p < 0.05$).

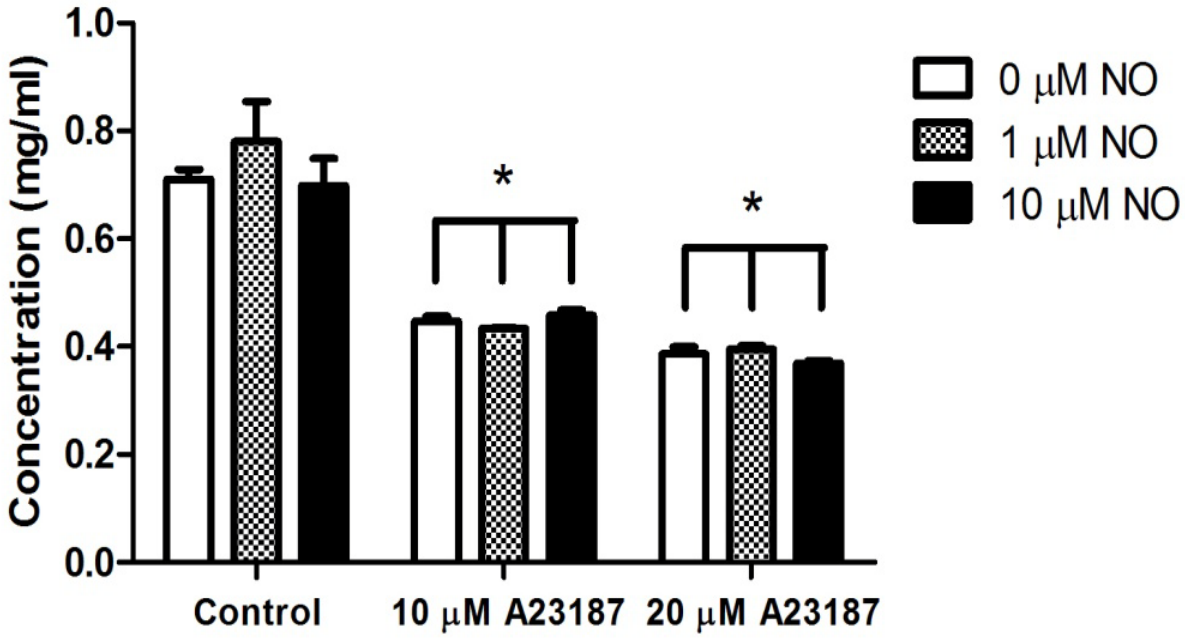

Figure 4-14. Total protein concentrations for L6 myotubes after 24 hours treatment with A23187 and/or DETA-NO. Values represent the mean ± SEM (n=3). *Significantly different from all control groups ($p < 0.05$). Significant main effect of A23187 treatment ($p < 0.0001$).

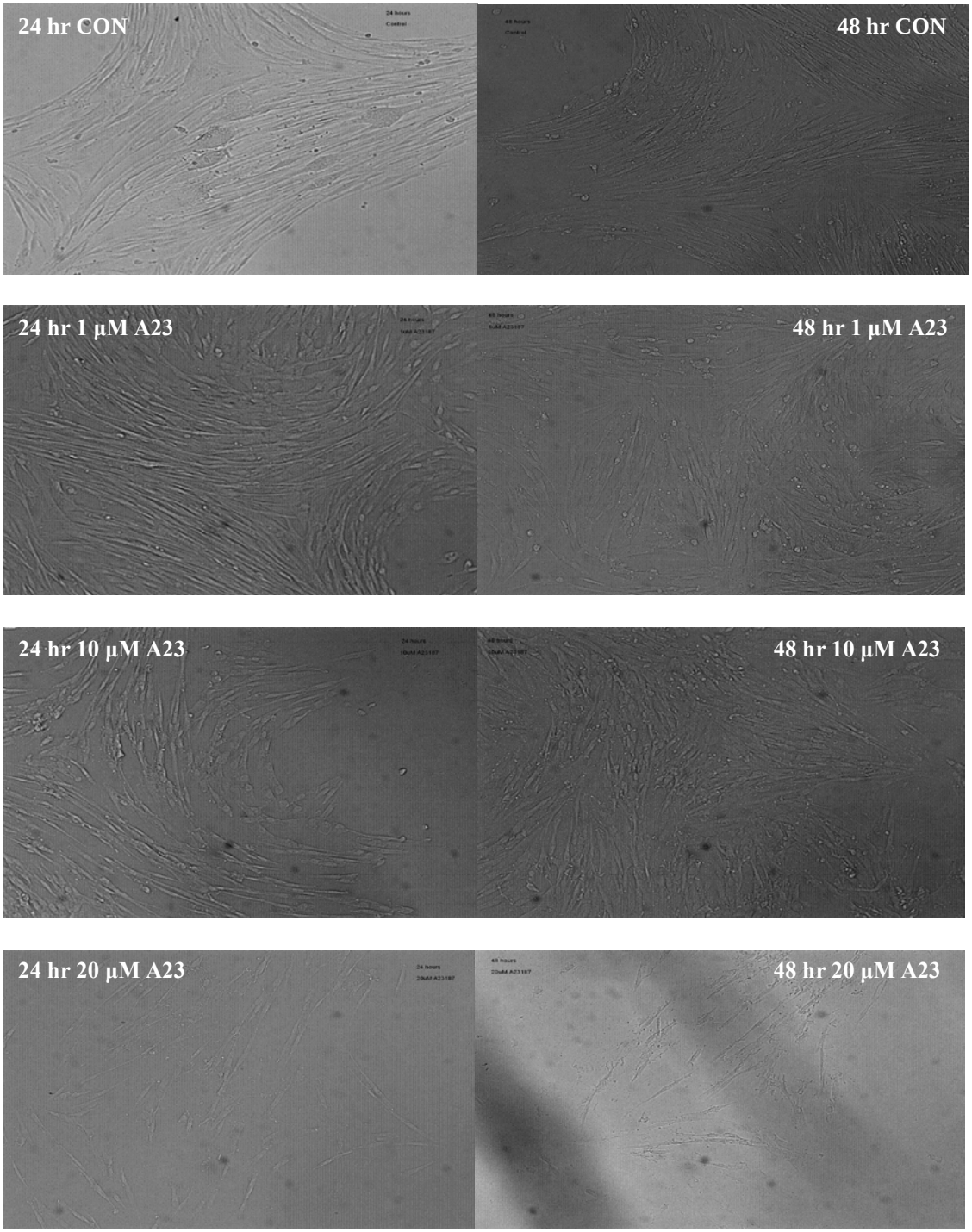

Figure 4-15. Representative images of L6 myotubes after 24 and 48 hours treatment with A23187. Left column represents 24 hours treatment. Right column represents 48 hours treatment. Top row represents control groups (DMSO only). Second row represents groups treated with 1 µM A23187. Third row represents groups treated with 10 µM A23187. Fourth row represents groups treated with 20 µM A23187.

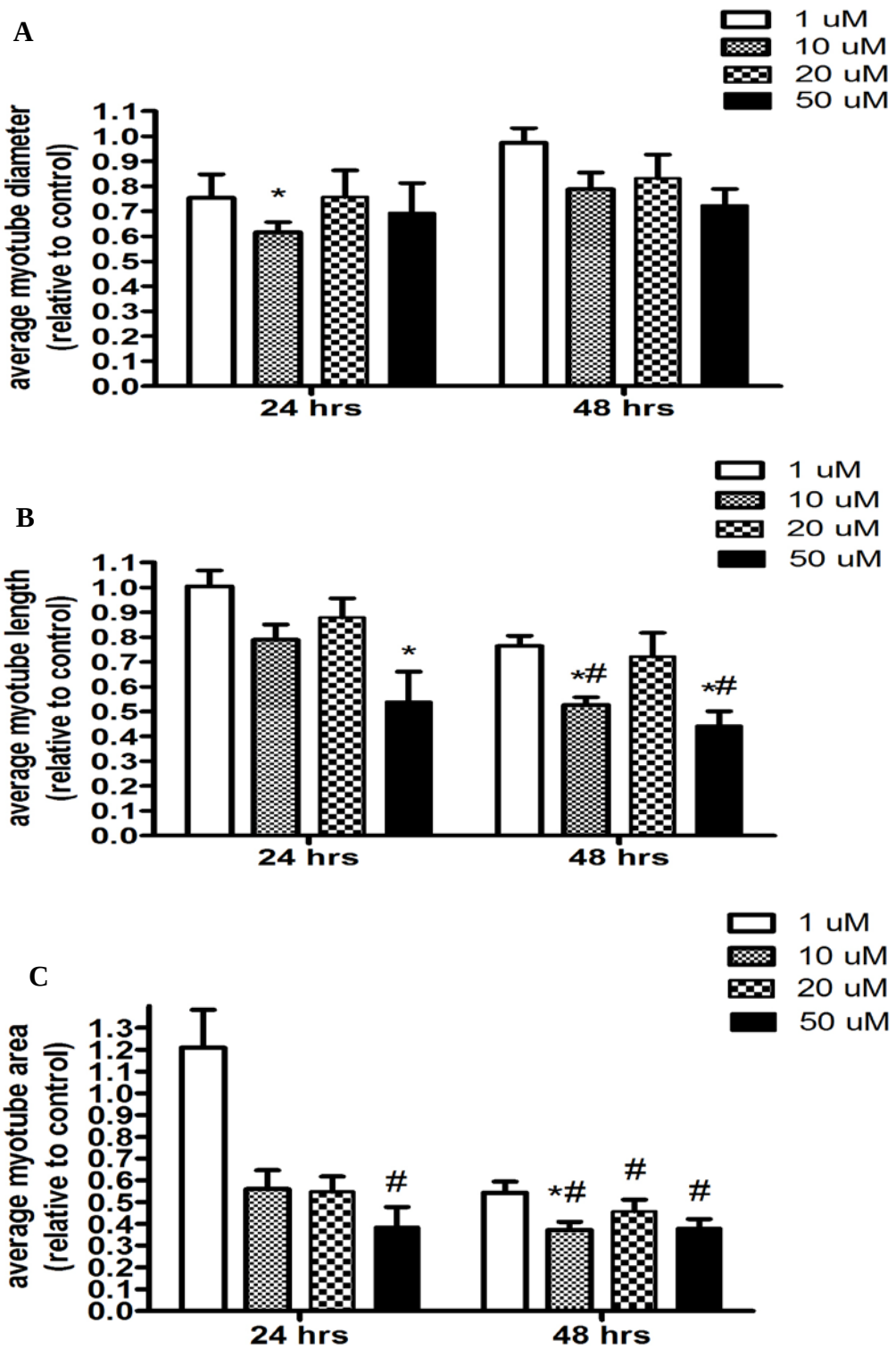

Figure 4-16. Image analysis of L6 myotubes after 24 and 48 hours treatment with A23187. A) Average myotube diameter. B) Average myotube length. C) Average myotube area. Values represent the mean ± SEM (n=7-10). *Significantly different from untreated control. #Significantly different from 24 hours of 1 µM A23187.

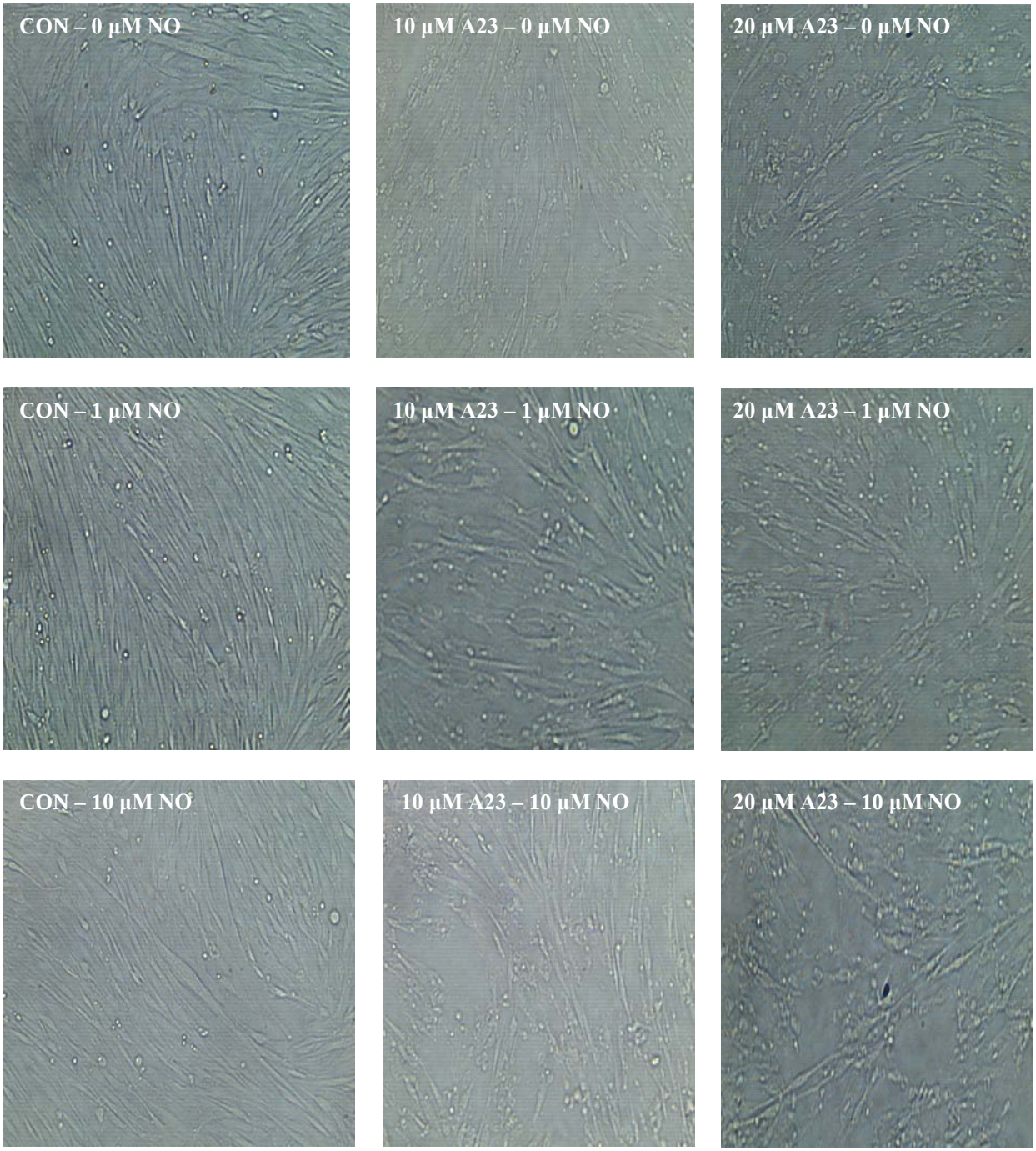

Figure 4-17. Representative images of L6 myotubes after 24 hours treatment with A23187 and/or DETA-NO. Left column represents control cells – no A23187. Middle column represents cells treated with 10 µM A23187. Right column represents cells treated with 20 µM A23187. Top row represents cells without NO treatment. Middle row represents cells concurrently treated with 1 µM NO. Bottom row represents cells concurrently treated with 10 µM NO.

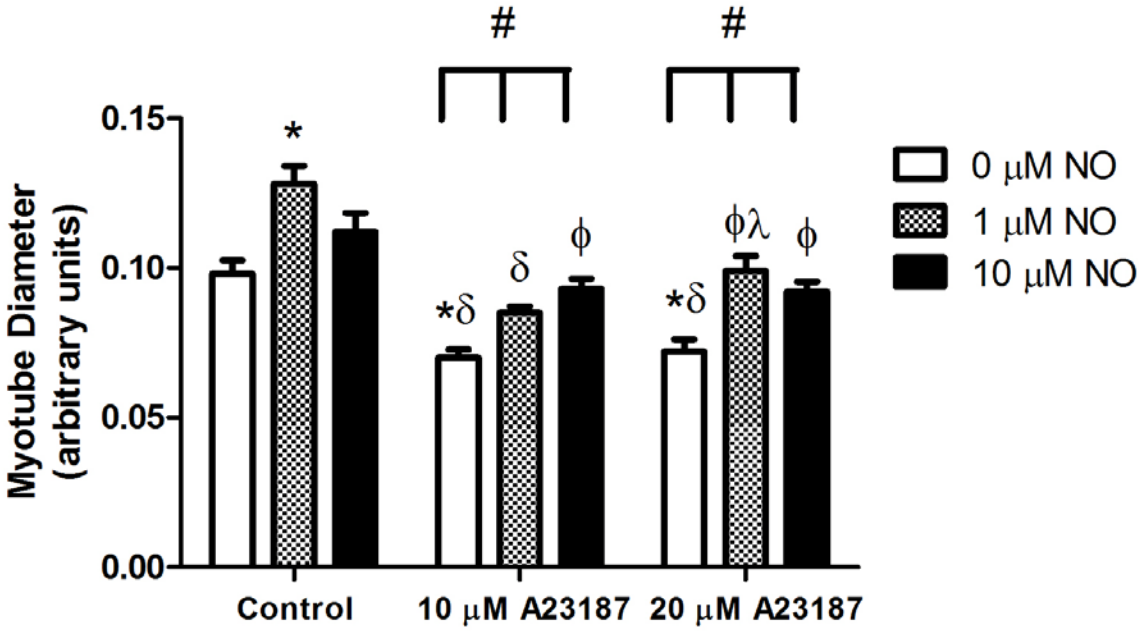

Figure 4-18. Image analysis of L6 myotube diameter after 24 hours treatment with A23187 and/or DETA-NO. Values represent the mean ± SEM (n=28-42). *Significantly different from control at 0 μM NO ($p < 0.05$). $^{\#}$Significantly different from control at 1 μM NO ($p < 0.05$). $^{\delta}$Significantly different from control at 10 μM NO ($p < 0.05$). $^{\varphi}$Significantly different from 10 μM A23187 + 0 μM NO ($p < 0.05$). $^{\lambda}$Significantly different from 20 μM A23187 + 0 μM NO ($p < 0.05$). Significant main effect of A23187 treatment ($p < 0.0001$). Significant main effect of NO treatment ($p < 0.0001$).

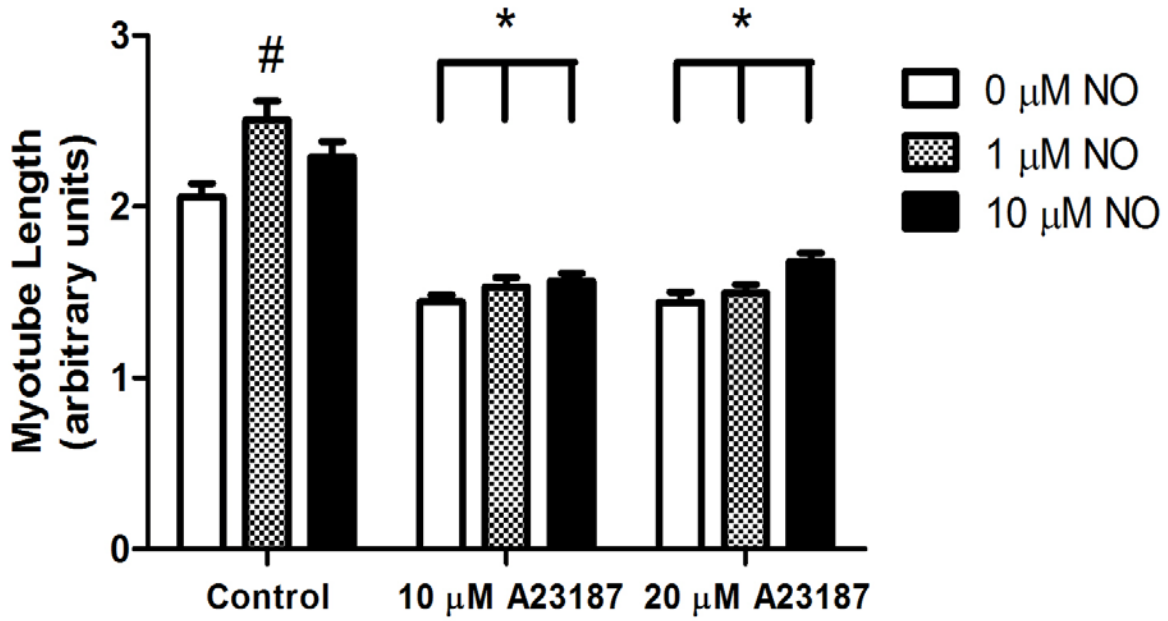

Figure 4-19. Image analysis of L6 myotube length after 24 hours treatment with A23187 and/or DETA-NO. Values represent the mean ± SEM (n=28-42). *Significantly different from all controls ($p < 0.05$). #Significantly different from control at 0 μM NO ($p < 0.05$). Significant main effect of A23187 treatment ($p < 0.0001$). Significant main effect of NO treatment ($p=0.0008$). Significant interaction between A23187 and NO ($p=0.02$).

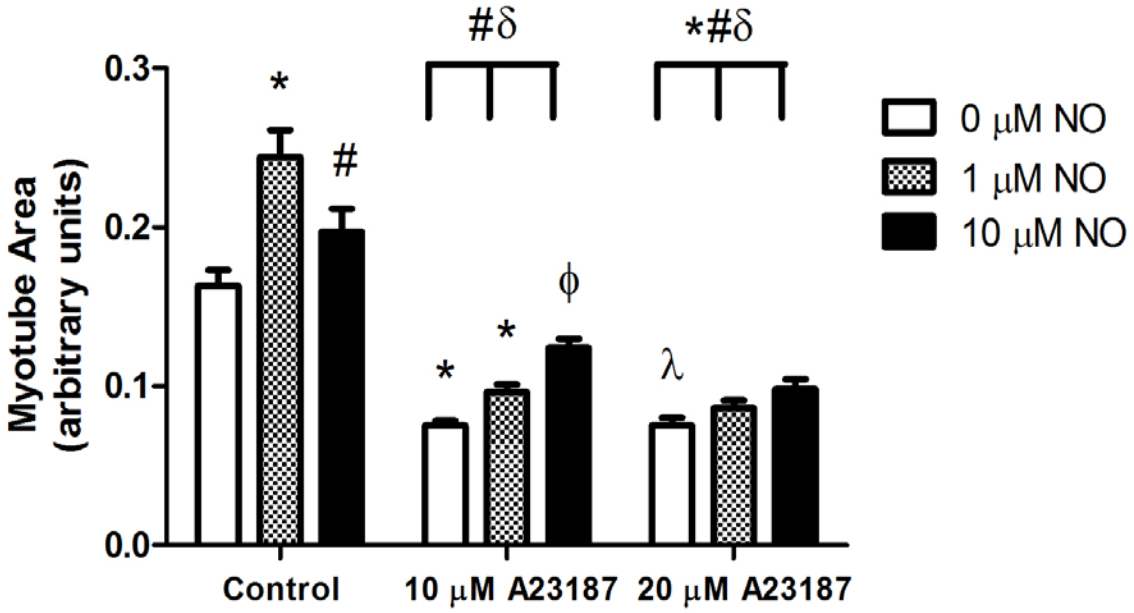

Figure 4-20. Image analysis of L6 myotube area after 24 hours treatment with A23187 and/or DETA-NO. Values represent the mean ± SEM (n=28-42). *Significantly different from control at 0 μM NO ($p < 0.05$). $^{\#}$Significantly different from control at 1 μM NO ($p < 0.05$). $^{\delta}$Significantly different from control at 10 μM NO ($p < 0.05$). $^{\varphi}$Significantly different from 10 μM A23187 + 0 μM NO ($p < 0.05$). $^{\lambda}$Significantly different from 10 μM A23187 + 10 μM NO ($p < 0.05$). Significant main effect of A23187 treatment ($p < 0.0001$). Significant main effect of NO treatment ($p < 0.0001$). Significant interaction between A23187 and NO ($p=0.0009$).

CHAPTER 5
DISCUSSION

Main Findings

This study demonstrated the dose-dependent effects of NO on calpain proteolysis of intermediate filaments in skeletal muscle myotubes during a Ca^{2+} challenge connected the changes in molecular markers of calpain proteolysis and proteasome activity with myotube atrophy (loss of size and/or total protein) during a Ca^{2+} challenge and exogenous NO administration.

Treatment with A23187 significantly increased the cleavage of talin, a protein known to be degraded by calpains, while treatment with PAPA-NO had a significant protective effect that varied with the doses of A23187 and PAPA-NO administered. The effects of A23187 on talin cleavage and the protective effects of PAPA-NO were independent of other molecular markers of proteolysis. Also, treatment with A23187 caused significant loss of cellular protein and myotube size, while DETA-NO prevented loss of myotube size during treatment with A23187 at certain dose combinations. These data demonstrate that NO can protect against calpain proteolysis and calpain-induced myotube atrophy during a Ca^{2+} challenge in L6 myotubes.

A23187 Causes Degradation of Intermediate Filaments by Calpains Independent of Proteasome Activity

We hypothesized that elevation of intracellular Ca^{2+} by treatment with A23187 would cause increased proteolysis of intermediate filaments (e.g. talin) by calpain and increased markers of proteasome activation (e.g. FOXO3a, MAFbx). We found that treatment with A23187 does cause increased proteolysis of the intermediate filaments by calpains, but this effect appears to be independent of proteasome activation.

Calpains are known to cleave the intermediate filament talin, leaving a 190-kDa fragment that is distinguishable by Western blotting from the 235-kDa intact protein (19). Treatment with

A23187 significantly increased calpain proteolysis of intermediate filaments, as measured by ratio of cleaved/intact talin protein (Figure 4-1). This effect was dose-dependent, as incrementally increasing A23187 was associated with an apparent, yet not always statistically significant, incremental increase in talin cleavage (Figure 4-1). Treatment with 10 µM and 20 µM A23187 caused statistically significant increases in cleavage (Figure 4-1, 4-2). Our results are consistent with evidence from C2C12 myoblasts that A23187 increases talin proteolysis (19). Although in our first experiment the increase in cleavage was not statistically significant with 10 µM A23187 (Figure 4-1), we expected that with a higher number of samples it would be. Therefore we continued experiments with both 10 µM A23187 and 20 µM A23187, and in our second experiment cells treated with 10 µM A23187 did show more cleavage than controls (Figure 4-2). Talin cleavage is an indirect measure of calpain activity that has been accepted in the literature as a measure of calpain proteoloysis (19, 42). However, in order to test that the talin cleavage was caused by calpains, we administered calpastatin, a known specific inhibitor of calpains I and II, to cells treated with 20 µM A23187 (with and without NO). With calpastatin blocking calpain activity, talin cleavage dropped dramatically for all groups (Figure 4-3), which suggests that the talin cleavage seen in response to A23187 treatment is in fact the result of calpain proteolysis.

Although we saw significant increases in calpain proteolysis, we did not observe concurrent changes in markers of proteasome activity in response to A23187 treatment. We chose to measure markers of proteasome activity in an attempt to connect calpain proteolysis of intermediate filaments with overall proteasome degradation. Previous research has demonstrated that cleavage of intermediate filaments and myofibrillar release by calpains precedes degradation by the proteasome (14, 27, 36). Recent research has also suggested that calpain activity is

necessary for proteasome action in the rat diaphragm (31). We measured phospho-Akt/total Akt, phospho-FOXO3a, and MAFbx protein expression for the three experiments designed to test specific aim 1. Increased Akt activation via phosphorylation by PI3K has been shown to be sufficient alone to downregulate the acitivty of proteasome E3 ligases MAFbx and MuRF1 (4, 29). However, phospho-Akt suppression of MAFbx and MuRF1 expression is dependent upon FOXO transcription factors (4, 29, 33). Unphosphorylated FOXO proteins are active and locate to the nucleus where they can stimulate E3 ligase transcription (40). Phospho-Akt inactivates FOXO proteins (including FOXO3a) by phosphorylation, which causes them to be translocated away from the nucleus and into the cytosol, where phospho-FOXO proteins are targeted by the proteasome for degradation (25, 40). Thus, if A23187 were causing proteasome activity, we would expect to see decreases in both phospho-Akt and phospho-FOXO3a expression and an increase in MAFbx expression. However, we did not see any significant changes in these proteins with A23187 treatment alone and treatment with calpeptin (blocking calpains) had no significant effects (Figures 4-4, 4-6, 4-7, 4-9, 4-10, 4-12).

While the lack of significant increase in any of these proteins following A23187 treatment was surprising, there are a few possible explanations. First, it is possible that proteasome activity and changes in these proteins were missed at 60 minutes. We chose to harvest cellular protein after 60 minutes of incubation with A23187 based upon previous evidence that proteasome activity in L6 myotubes increases most rapidly during the first 40 minutes of incubation with A23187 and then continues to increase significantly for 120 minutes (21). Importantly, however, this study did not measure proteins involved in cellular signaling but rather overall proteasome activity by measuring degradation of a fluorescent substrate (21). Based on the little previous data that we had, we believed that 60 minutes would be sufficient time to see proteasome activity

but still brief enough not to miss evidence of the calpain cleavage that should precede it. Incubating for a longer period would have risked losing the cleaved talin protein to proteasome degradation, and since we were primarily concerned with calpain activity in this study, we chose to limit the time to 60 minutes. It is possible, then that proteasome activity was occurring but that the the molecular markers that we measured were not captured at 60 minutes.

Second, it is possible that proteasome activity was occurring but not via the inactive-Akt/FOXO/E3 ligase pathway. These proteins, while associated with skeletal muscle atrophy, are only a few of the myriad of indirect measurements of proteolytic activity. We chose to study this pathway based on previous work that has shown calpain activity inhibiting Akt signaling in skeletal muscle (31) and previous data from our laboratory that has shown a significant relationship between Akt signaling and NO in skeletal muscle (7). We chose to measure MAFbx as a representative of E3 ligases because of its predominance in the literature and availability of a reliable antibody. However, it is possible that other E3 ligases, such as MuRF1, would have yielded a different result.

Third, it is possible that in L6 myotubes, proteolysis by calpains and protesomes have a different relationship than in other skeletal muscle cell lines. L6 myotubes differentiate into mature myotubes with striations, but they do not have functional sarcomeres and do not contract. We chose this cell line because other cell lines, such as C2C12s, would not withstand the Ca^{2+} challenge as mature myotubes because they would contract, dislodge from the plate, and die. We attempted to use both cell lines in initial experiments to confirm that C2C12 myotubes were not a viable choice for this study, and this is likely why the only previous study of the effects of A23187 and NO on skeletal muscle cells in culture was done in myoblasts (19). While L6 myotubes do not have functional sarcomeres, they do express all proteins that we studied, as

evidenced by our data. It is still possible, however, that the sequence of proteolytic events (requisite calpain cleavage followed by proteasome action) is different for this cell line. The one study previously mentioned that measured proteasome activity in response to A23187 did not measure any markers of calpain activity (21). Therefore, it is possible that calpain and proteasome activity do not occur in the same sequence or with the same timing in L6 myotubes as in other cell lines. Considerably more research would need to be done on this subject before assessing how likely this possibility is, however, it would explain the consistency of our results showing calpain activity changes without concomitant changes in the other atrophy markers.

Exogenous NO Prevents Degradation of Intermediate Filaments by Calpains Independent of Proteasome Activity

We hypothesized that exogenous NO administration would attenuate calpain proteoloysis and proteasome activity after treatment with A23187. We found that NO does protect against proteolysis of the intermediate filaments by calpains, but this effect appears to be independent of proteasome activity and is dose-dependent.

NO has been proposed as a potential regulator of calpain activity in various tissues by a small number of previous studies (5, 19, 22, 42). We used two doses of PAPA-NO (1 µM and 10 µM) crossed with the two doses of A23187 that appeared to induce cleavage of the intermediate filaments by calpains (10 µM and 20 µM) to test the ability of NO to protect against calpains during a Ca^{2+} challenge. We also used L-NMMA, an inhibitor of endogenous NO release, to further assess the role of NO. Both 1 µM and 10 µM PAPA-NO were able to significantly attenuate talin cleavage by calpains after treatment with 10 µM A23187 (Figure 4-2). However, only 10 µM PAPA-NO was able to attenuate talin cleavage after treatment with 20 µM A23187 (Figure 4-2). Treatment with L-NMMA resulted in increased talin cleavage as compared to untreated controls but did not have a significantly different effect than treatment

with A23187 alone (Figure 4-2). These results suggest that NO does mediate calpain activity during a Ca^{2+} challenge, but that the dose of NO required to protect intermediate filament proteins from degradation is dependent upon the level of Ca^{2+}. Since NO can have either positive or negative effects throughout the cell depending on the dose, it is important to note that a dose as low as 1 µM PAPA-NO had a significant protective effect and that 10 µM PAPA-NO protected at both doses of A23187 but was not required for protection at the relatively lower dose of A23187. And while treatment with L-NMMA did not produce an increase in talin cleavage at a level that reached statistical significance at $n=6$ and $p < 0.05$, it appears that blocking endogenous NO with L-NMMA could cause a slight increase (Figure 4-2). Because this study was primarily concerned with exogenous NO as a potential mediator, we did not study L-NMMA or other NO blockers alone. However, future experiments exploring the the effect of endogenous NO on calpain proteolysis of intermediate filaments would be useful in determining if endogenous NO could protect skeletal muscle from calpain proteolysis or if exogenous NO is required in therapeutic doses as studied here. One previous study has examined endogenous NO release on calpain activity in a mechanical strain model with positive results (42). Finally, we showed that NO did not attenuate calpain activity as significantly and universally as calpeptin and that NO + calpeptin treatment was not different from treatment with calpeptin alone (Figure 4-3). This is likely due to the potency of the calpeptin and its efficacy as a blocker of both calpain I and calpain II.

Although NO had protective effects on the intermediate filaments by inhibiting proteolysis by calpains, treatment with NO had few significant effects on markers of proteasome activation. If NO was protecting against proteasome activity, we would expect to see increased Akt

phosphorylation and phospho-FOXO3a expression and decreased MAFbx expression. However, our data did not support this.

Akt phosphorylation increased with treatment with 10 µM A23187 + all doses of NO or L-NMMA, but there were no differences among these groups (Figure 4-5). Thus, NO did not affect Akt phosphorylation in our study. This somewhat conflicts with evidence published by our lab that shows eNOS knockout mice treated with 0.4 µM A23187 have dramatically reduced Akt phosphorylation, which is restored by PAPA-NO administration (7). However, this study used very low levels of A23187 and was conducted in a different model, so comparison is difficult. Since Akt phosphorylation did increase with 10 µM A23187 but not with any of the treatment groups at the higher dose of A23187, it may be that the effect of A23187 on Akt phosphorylation is dose and/or time-dependent. Dose-dependence is seen in many different physiological molecules, including NO, so it is not unrealistic to consider that Akt phosphorylation could be triggered by certain levels of intracellular Ca^{2+} but could be unchanged (as in our study) or even reversed by other levels.

Phospo-FOXO3a expression paradoxically increased with 10 µM A23187 alone and with 1 µM PAPA-NO but did not change in any other group (Figure 4-8). This result is difficult to explain, and in light of the lack of significant changes in phospho-FOXO3a throughout our study (Figures 4-7, 4-8, 4-9) it may be that this protein is not affected by A23187, calpain activity, or NO in L6 myotubes. And, as previously stated, it is possible that calpain and proteasome activity do not occur in the same sequence or with the same timing in L6 myotubes as they do in other cell lines.

MAFbx expression paradoxically decreased with 20 µM A23187 alone and with 20 µM A23187 + either dose of PAPA-NO (Figure 4-11). No other significant changes in MAFbx were

seen throughout our study (Figures 4-10, 4-11, 4-12). Again, this result is difficult to explain, and it may be that this protein is not affected by A23187, calpain activity, or NO in L6 myotubes. And, as previously stated, it is possible that calpain and proteasome activity do not occur in the same sequence or with the same timing in L6 myotubes as they do in other cell lines.

Although there were few significant differences in Akt phosphorylation, phospho-FOXO3a, or MAFbx expression with A23187 and NO treatments, it should be noted that the lack of changes is remarkably consistent, and that we would expect this to be the case if this pathway was either not captured at the 60 minute treatment end or not active in our L6 myotubes in this atrophy model. Since we expected these proteins to be expressed together and to work in concert, relative consistency in their lack of change among treatment conditions is not especially surprising and further supports the idea that proteasome activity was either missed by our 60 minute treatment or that the coupling of calpain and proteasome activity is not the same in L6 myotubes as it is in other cells.

High Doses of A23187 Cause L6 Myotube Atrophy

We hypothesized that elevation of intracellular Ca^{2+} by treatment with A23187 causes myotube atrophy. This is the first study to our knowledge to attempt to connect the markers of calpain proteolysis with myotube atrophy, and we found that the same doses of A23187 that increase calpain activity also cause cause myotube atrophy over 24-48 hours. After 24 hours of treatment, 5 µM, 10 µM, and 20 µM doses of A23187 caused loss of total protein (Figure 4-13). This is particularly important in light of our data showing that proteolysis by calpains is increased with 60 minutes treatment with 10 µM and 20 µM A23187 (Figures 4-1, 4-2). After 24 hours of treatment, there was little change in myotube diameter, length, or area with any dose of A23187 below 50 µM (Figure 4-15). However, after 48 hours, cells treated with 10 µM and 20 µM A23187 (as well as 50 µM) showed decreased myotube area (Figure 4-15). The loss of

protein by 24 hours and loss of myotube area by 48 hours are evidence of A23187-induced myotube atrophy. Furthermore, we can connect the increase in calpain proteolysis of the intermediate filaments seen in the first 60 minutes of treatment (Figure 4-1) with this evidence of atrophy at the same doses (Figures 4-13 and 4-15) over 24 and 48 hours and conclude that the calpain proteolysis induced by A23187 is a sign of atrophy, not simply cellular remodeling.

Exogenous NO Protects L6 Myotubes from A23187-Induced Atrophy

We hypothesized that exogenous NO would attenutate myotube atrophy after treatment with A23187, and we found that, while it did not attenuate the loss of total protein associated with A23187 treatment, exogenous NO did attenuate loss of myotube size at certain dose combinations. When cells were treated with DETA-NO along with A23187, protein degradation decreased with A23187 treatment but was not affected by NO after 24 hours (Figure 4-14). The lack of protection by NO was not expected, especially in light of the preservation of myotube size discussed below. It is possible that NO does not protect against total protein loss during a Ca^{2+} challenge. However, a significant number of cells were lost during the process of stopping treatment, washing with PBS, image capturing, and harvesting. This likely affected the results of this experiment and may have contributed to the lack of significant results.

Although it did not preserve total cellular protein, concurrent treatment with NO did preserve myotube size. For cells treated with 10 µM A23187, both 1 µM and 10 µM DETA-NO preserved myotube diameter to the level of untreated controls; 10 µM DETA-NO also significantly increased myotube diameter as compared to cells treated with 10 µM A23187 alone. Additionally, 10 µM DETA-NO preserved myotube area to a level similar to untreated controls; myotube area for these cells was significantly greater than for those treated with 10 µM A23187 alone. For cells treated with 20 µM A23187, 1 µM DETA-NO significantly increased myotube diameter as compared to 20 µM A23187 alone, and both 1 µM DETA-NO or 10 µM

DETA-NO resulted in significantly greater myotube diameter than the lower dose 10 μM A23187 alone, indicating partial protection of myotube diameter. However, NO had no protective effects on myotube area during the higher dose A23187 treatment. These effects on myotube size indicate that NO can protect myotubes from loss of size but that the effects are dependent upon the severity of the Ca^{2+} challenge.

We conclude that NO protects L6 myotubes from A23187-induced atrophy, as measured by changes in myotube size, but that the dose of NO required to protect the myotubes is dependent upon the dose of A23187 and that the deleterious effects of higher levels of intracellular Ca^{2+} may be too much for NO to counteract. These results agree with our molecular markers results, which showed that NO protects against calpain cleavage of intermediate filaments at the same doses of A23187 and NO. Thus, we conclude that the attenuation of calpain cleavage of intermediate filaments is evidence of myotube atrophy, not simply cellular remodeling and that NO can protect L6 myotubes from calpain-induced atrophy.

Limitations and Future Directions

This study was limited by several factors, the first of which is the use of an ionophore. Using A23187 as our independent variable to raise intracellular Ca^{2+} is not a physiological stimulus of Ca^{2+} influx. A23187 is an ionophore that allows divalent cations, such as Ca^{2+} to cross the cell membrane and raise intracellular concentrations. Although this ionophore is widely used in cell culture as a method of increasing intracellular Ca^{2+}, it does have other effects on the cell, such as inhibiting oxidative phosphorylation and acting as an antibiotic. We do not believe that the secondary effects of the ionophore significantly compromise our study results because the effects should not impact atrophy or associated signaling in non-contracting cells.

Second, this study was limited by the use of indirect measures of proteolysis. Talin cleavage was used as an indirect marker of calpain activity. However, this is not uncommon in

the literature, and our results showing calpeptin reversing the talin cleavage support the assumption that talin cleavage is representative of calpain activity. Akt (de-)phosporylation is limited because alone it would be a very indirect indicator of proteolytic activity. However, we also measured two of the proteins downstream of Akt: FOXO and MAFbx. Using phospho-FOXO3a was somewhat indirect as well because we assume that loss of phospho-FOXO3a represents de-phosphorylation and translocation to the nucleus. However, we also measured MAFbx, the transcription of which is upregulated by FOXO3a. The measurement of only MAFbx expression to represent E3 ligases is also limiting. Future studies should isolate nuclear and cytosolic fractions to measure FOXO3a/FOXO3a~P and should also measure MuRF1 expression.

Third, this study was limited in that we could only examine certain timepoints as "snapshots" of what was occurring in the myotubes. It is highly possible that some changes in proteins measured were missed because they were either degraded during the 60 minute treatment period or not yet activated or elevated. A low number of samples also compromised our ability to elucidate the cell signaling occurring in our study. Future studies should examine different time points and increase the number of samples taken.

Finally, this study is limited as are all *in vitro* cell culture studies by our inability to apply these results directly to a whole organism. However, *in vitro* studies such as this one are necessary to study the mechanisms behind clinical problems like skeletal muscle atrophy with maximal experimental control and minimal influence of other physiological factors.

Conclusions

We conclude that elevation of intracellular Ca^{2+} by treatment with A23187 causes increased proteolysis of intermediate filaments (e.g. talin) by calpain independent of proteasome activity and that exogenous NO administration attenuates calpain proteoloysis but not

proteasome activity after treatment with A23187. We further conclude that the increases in calpain activity induced by treatment with A23187 causes myotube atrophy and that exogenous NO protects L6 myotubes from A23187-induced atrophy.

LIST OF REFERENCES

1. **Bartoli M and Richard I.** Calpains in muscle wasting. *International Journal of Biochemistry and Cell Biology* 37: 2115-2133, 2005.

2. **Bechet D, Tassa A, Taillandier D, Combaret L, Attaix D.** Lysosomal proteolysis in skeletal muscle. *International Journal of Biochemistry and Cell Biology* 37: 2098-2114, 2005.

3. **Bergamini E.** Autophagy: A cell repair mechanism that retards aging and age-associated diseases and can be intensified pharmacologically. *Molecular Aspects of Medicine.* 27: 403-410, 2006.

4. **Bodine SC, Latres E, Baumhueter S, Lai VKM, Nunez L, Clarke B, Poueymirou WT, Panaro FJ, Na E, Dharmarajan K, Zhen-Qiang P, Valenzuela DM, DeChiara TM, Stitt TN, Yancopoulos GD, Glass DJ.** Identification of Ubiquitin Ligases Required for Skeletal Muscle Atrophy. *Science* 294: 1704-1708, 2001.

5. **Chohan PK, Singh RB, Dhalla NS, and Netticadan T.** L-arginine administration recovers sarcoplasmic reticulum function in ischemic reperfused hearts by preventing calpain activation. *Cardiovascular Research* 69: 152-163, 2006.

6. **Costelli P, Reffo P, Penna F, Autelli R, Bonelli G, Baccino FM.** Ca^{2+}-dependent proteolysis in muscle wasting. *International Journal of Biochemistry and Cell Biology,* 37: 2134-2146, 2005.

7. **Drenning JA, Lira VA, Soltow QA, Cannon CN, Valera LM, Brown DL, Criswell DS.** Endothelial nitric oxide synthase is involved in calcium-induced Akt signaling in mouse skeletal muscle. *Nitric Oxide* In Press, 2009.

8. **Du J, Wang X, Miereles C, Bailey JL, Debigare R, Zheng B, Price SR, and Mitch WE.** Activation of caspase-3 is an initial step triggering accelerated muscle proteolysis in catabolic conditions. *Journal of Clinical Investigations* 113: 115-123, 2004.

9. **Furano K & Goldberg AL.** The activation of protein degradation in muscle by Ca^{2+} or muscle injury does not involve a lysomsomal mechanism. *The Biochemical Journal* 237: 859-864, 1986.

10. **Gissel H.** The role of Ca^{2+} in muscle cell damage. *Annals of the New York Academy of Sciences* 1066: 166-180, 2005.

11. **Gissel H and Clausen T.** Excitation-induced Ca^{2+} influx and skeletal muscle cell damage. *Acta Physiologica Scandinavica* 171: 327-334, 2001.

12. **Glass DJ.** Molecular mechanisms modulating muscle mass. *Trends in Molecular Medicine* 9: 344-350, 2003.

13. **Glass DJ.** Skeletal muscle hypertrophy and atrophy signaling pathways. *International Journal of Biochemistry and Cell Biology* 37: 1974-1984, 2005.

14. **Goll DE, Thompson VF, Li H, Wei W, and Cong J.** The calpain system. *Physiological Reviews* 83: 731-801, 2003.

15. **Gomes MD, Lecker SH, Jagoe RT, Navon A, Goldberg AL.** Atrogin-1, a muscle-specific F-box protein highly expressed during muscle atrophy. *Proceedings of the National Academy of Sciences* 98: 14440-14445, 2001.

16. **Grune T, Merker K, Sandig G, and Davies KJ.** Selective degradation of oxidatively modified substrates by the proteasome. *Biochemical and Biophysical Research Communications* 305: 709-718, 2003.

17. **Hershko A, Ciechanover A.** The ubiquitin system. *Annual Reviews in Biochemistry* 67: 425-427, 1988.

18. **Jackman RW and Kandarian SC.** The molecular basis of skeletal muscle atrophy. *American Journal of Physiology Cell Physiology* 287: C834-C843, 2004.

19. **Koh TJ and Tidball JG.** Nitric oxide inhibits calpain-mediated proteolysis of talin in skeletal muscle cells. *American Journal of Physiology Cell Physiology* 279: C806-C812, 2000.

20. **Li YP, Chen Y, Li AS, and Reid MB.** Hydrogen peroxide stimulates ubiquitin-conjugating activity and expression of genes for specific E2 and E3 proteins in skeletal muscle myotubes. *American Journal of Physiology Cell Physiology* 285: C806-812, 2003.

21. **Menconi MJ, Wei W, Yang H, Wray CJ, Hasselgren PO.** Treatment of cultured myotubes with the calcium ionophore A23187 increases proteasome activity via a CaMK II-caspase-calpain-dependent mechanism. *Surgery* 136: 135-142, 2004.

22. **Michetti M, Salamino F, Melloni E, and Pontremoli S.** Reversible inactivation of calpain isoforms by nitric oxide. *Biochemical and Biophysical Research Communications* 207: 1009-1014, 1995.

23. **Musial A and Elissa NT.** Inducible nitric-oxide synthase is regulated by the proteasome degradation pathway. *Journal of Biological Chemistry* 276: 24268-24273, 2001.

24. **Otani K, Han D, Ford E, Garcia-Roves PM, Ye H, Horikawa Y, Bell GI, Holloszy JO, and Polonsky KS.** Calpain system regulates muscle mass and glucose transporter GLUT4 turnover. *Journal of Biological Chemistry* 279: 20915-20920, 2004.

25. **Plas DR, Thompson CB.** Akt activation promotes degradation of tuberin and FOXO3a via the proteasome. *Journal of Biological Chemistry* 278: 12361-12366, 2003.

26. **Powers SK, Kavazis AN, and DeRuisseau KC.** Mechanisms of disuse muscle atrophy: role of oxidative stress. *American Journal of Physiology Regulatory, Integrative, and Comparative Physiology* 288: 337-344, 2005.

27. **Powers SK, Kavazis AN, & McClung JM.** Oxidative stress and disuse muscle atrophy. *Journal of Applied Physiology* 102: 2389-97, 2007.

28. **Sacheck JM, Ohtsuka A, McLary SC and Goldberg AL.** IGF-1 stimulates muscle growth by suppressing protein breakdown and expression of atrophy-related ubiquitin ligases, atrogin-1 and MuRF1. *American Journal of Physiology Endocrinology and Metabolism* 287: E591-601, 2004.

29. **Sandri M, Sandri C, Gilbert A, Skurk C, Calabria E, Picard A, Walsh K, Schiaffino S, Lecker SH and Goldberg AL.** FOXO transcription factors induce the atrophy-related ubiquitin ligase atrogin-1 and cause skeletal muscle atrophy. *Cell* 117: 399-412, 2004.

30. **Senf SM, Dodd SL, McClung JM and Judge AR.** Hsp70 overexpression inhibits NF-{kappa}b and FOXO3a transcriptional activities and prevents skeletal muscle atrophy. The *FASEB Journal* 22: 3836-45, 2008.

31. **Smith IJ and Dodd SL.** Calpain activation causes a proteosome dependent increase in protein degradation and inhibits the Akt signaling pathway in rat diaphragm muscle. *Experimental Physiology* 92:561-73, 2007.

32. **Spencer MJ, Lu B, and Tidball JG.** Calpain II expression is increased by changes in mechanical loading of muscle in vivo. *Journal of Cellular Biochemistry* 64: 55-66, 1997.

33. **Stitt TN, Drujan D, Clarke BA, Panaro F, Timofeyva Y, Kline WO, Gonzalez M, Yancopoulos GD and Glass DJ.** The IGF-1/PI3K/Akt pathway prevents expression of muscle atrophy-induced ubiquitin ligases by inhibiting foxo transcription factors. *Molecular Cell* 14: 395-403, 2004.

34. **Taillander D, Aurousseau E, Meynial-Davis D, Bechet D, Ferrara M, Cottin P, Ducastataing A, Bigard X, Guezennec CY, Schmid HP, and Attaix D.** Coordinate activation of lysosomal, Ca^{2+}-activated and ATP-ubiquitin-dependent proteases in the unweighted rat soleus muscle. *The Biochemical Journal* 316: 65-72, 1996.

35. **Taillander D, Combaret L, Pouch MN, Samuels SE, Bechet D, Attaix D.** The role of ubiquitin-proteasome-dependent proteolysis in the remodeling of skeletal muscle. *Proceedings of the Nutrition Society* 63: 357-361, 2004.

36. **Tidball JG and Spencer MJ.** Expression of a calpastatin transgene slows muscle wasting and obviates changes in myosin isoform expression during murine muscle disuse. *Journal of Physiology* 545: 819-828, 2002.

37. **Tischler ME, Rosenberg S, Satarug S, Henriksen EJ, Kirby CR, Tome M, and Chase P.** Different mechanisms of increased proteolysis in atrophy induced by denervation or unweighting of rat soleus muscle. *Metabolism* 39: 756-763, 1990.

38. **Thompson VF, Lawson K, and Goll DE.** Effect of μ-calpain on m-calpain. *Biochemical and Biophysical Research Communications* 267: 495-499, 2000.

39. **Vassilakopoulos T, Deckman G, Kebbewar M, Rallis G, Harfouche R, and Hussain SNA.** Regulation of nitric oxide production in limb and ventilatory muscles during chronic exercise training. *American Journal of Physiology Lung Cell Molecular Physiology* 284: L452-L457, 2002.40. **Van der Heide LP, Hoekman MF, Smidt MP.** The ins and outs of FOXO shuttling: mechanisms of FOXO translocation and transcriptional regulation. *The Biochemical Journal* 380: 297-309, 2004.

41. **Wray CJ, Mammen JM, Hershko DD, Hasselgren PO.** Sepsis upregulates the gene expression of multiple ubiquitin ligases in skeletal muscle. *International Journal of Biochemistry & Cell Biology* 35: 698-705, 2003.

42. **Zhang JS, Kraus WE, and Truskey GA.** Stretch-induced nitric oxide modulates mechanical properties of skeletal muscle cells. *American Journal of Physiology Cell Physiology* 287: 292-299, 2004.

BIOGRAPHICAL SKETCH

Elizabeth Henderson Zeanah is the daughter of William Ross Zeanah, M.D. and Sharon Cook Zeanah. Ms. Zeanah was born in Houston, Texas and raised in Gainesville, Florida, where she attended Eastside High School and graduated from the International Baccalaureate (IB) program. Ms. Zeanah then moved to Los Angeles, California, where she received a Bachelor of Science in Kinesiology from the University of Southern California (USC) and a minor in Public Health from the USC Keck School of Medicine in 2006. While at USC, Ms. Zeanah assisted with projects in glucose transport and lipid metabolism in skeletal muscle under the direction of Dr. Lorraine Turcotte. She was also a three-year letterwinner, PAC-10 champion, and NCAA Championships finalist as a scholarship athlete on the USC women's rowing team. After graduating from USC, Ms. Zeanah chose to puruse a Master of Science in applied physiology and kinesiology with a concentration in exercise physiology at the University of Florida and to continue research in skeletal muscle physiology. For the next three years, Ms. Zeanah conducted *in vitro* skeletal muscle research in the Molecular Physiology Laboratory directed by Dr. David Criswell. During her third year, she also began doctoral program studies in exercise physiology and conducted clinical and translational cardiovascular research in the Cardiovascular Physiology Laboratory under the direction of Dr. Randy Braith. After obtaining her Master of Science degree from the University of Florida in 2009, Ms. Zeanah plans to continue her studies and cardiovascular research in pursuit of a Doctor of Philosophy degree.